Image Recognition of Dyed Fibers and Component Analysis of Cigarette Paper Based on Hue, Saturation, and Value (HSV) Threshold Segmentation

Jinsheng Rui,[a] Min You,[a] Haiying Wei,[a] Yueyue Wang,[b] Xinke Yan,[b] Lidong Zhou,[b] Chengwen Zhu,[a,*] and Hao Ren [b,*]

** Corresponding authors: zhucw@jszygs.com (Chengwen Zhu); renhao@njfu.edu.cn (Hao Ren)*

DOI: 10.15376/biores.21.2.4408-4435

GRAPHICAL ABSTRACT

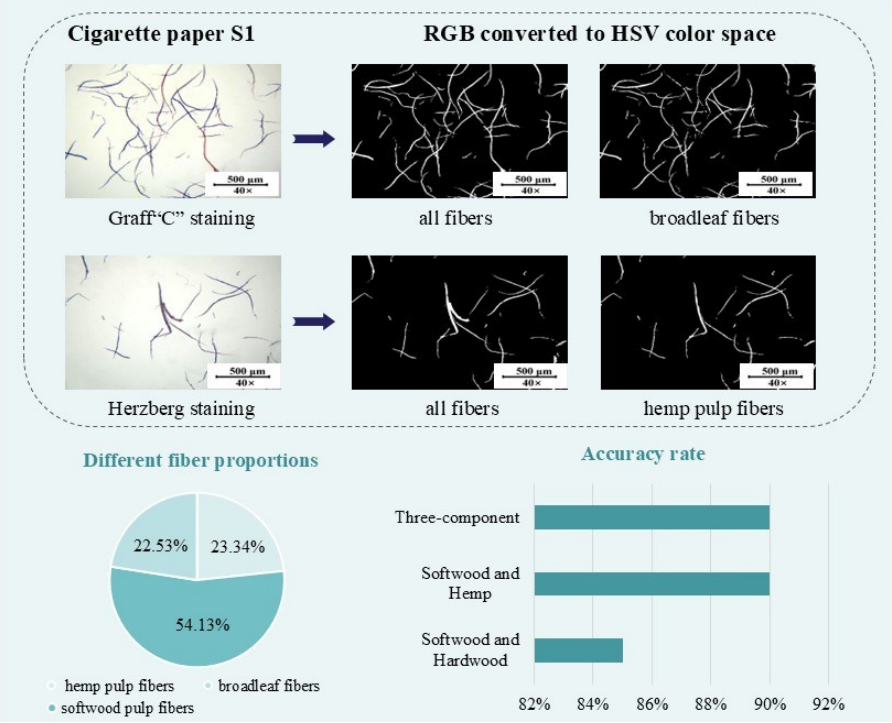

Image Recognition of Dyed Fibers and Component Analysis of Cigarette Paper Based on Hue, Saturation, and Value (HSV) Threshold Segmentation

Jinsheng Rui,[a] Min You,[a] Haiying Wei,[a] Yueyue Wang,[b] Xinke Yan,[b] Lidong Zhou,[b] Chengwen Zhu,[a,*] and Hao Ren [b,*]

Traditional fiber component analysis combining Herzberg and Graff "C" staining methods achieves high accuracy but relies on manual fiber length measurement using an ImageJ software, making it cumbersome and subjective. This study developed a MATLAB-based image preprocessing approach utilizing HSV color space transformation and color threshold segmentation to achieve precise extraction of different fibers from stained microscopic images. Experiments employed four two-component and two three-component mixed slurry samples to compare accuracy and efficiency against the ImageJ method. Optimal color rendering was attained with saturation and lightness gain factors of 1.5 and 1.1 after Herzberg staining and 2.0 and 1.1 after Graff "C" staining. The new method matched ImageJ's accuracy while significantly improving processing efficiency. Applied to commercial cigarette paper, it accurately identified fiber components, consistent with raw material data. Integrating staining techniques with image recognition maintains analytical precision while substantially boosting detection speed. This approach provides an efficient high-throughput solution for cigarette paper fiber analysis with clear industrial application potential.

DOI: 10.15376/biores.21.2.4408-4435

Keywords: Combination of the dyeing methods; Image recognition; HSV color space; Threshold segmentation

Contact information: a: China Tobacco Jiangsu Industrial Co., Ltd., Nanjing 210019, China; b: Jiangsu Provincial Key Lab of Pulp and Paper Science and Technology, Nanjing Forestry University, Nanjing, Jiangsu Province, 210037, China;
** Corresponding authors: zhucw@jszygs.com (Chengwen Zhu); renhao@njfu.edu.cn (Hao Ren)*

INTRODUCTION

Accurate analysis of fiber components in cigarette paper is crucial for regulating the combustion performance and smoke quality of cigarettes (Liu 2011; Chokshi *et al*. 2020). In previous studies, although the combined use of Herzberg (Sun and Zhang 2021) and Graff "C" (Li *et al*. 2023) stains with ImageJ software could distinguish fiber types based on color differences, the quantitative analysis relied on manual measurement of fiber length in ImageJ, with several bottlenecks including complex workflows, strong manual subjectivity, and low efficiency, making it difficult to meet industrial analysis requirements. As the tobacco industry shifts toward intelligent and refined production, developing automated and high-efficiency fiber analysis technology has become an urgent need.

Digital image processing (Vyas *et al*. 2018; Newell 2020) technology has already shown great potential in medical microscopy (Robertson *et al*. 2016; Zhang and Dong 2016), materials science (Xing *et al*. 2019; Abdelkader 2022), and other fields. This is due to its fast and objective characteristics, providing a new approach to solve this challenge by using methods such as color space conversion (Jraissati and Douven 2018; Cinko and Becerir 2024), threshold segmentation (Zortea *et al*. 2017; Abd Elaziz *et al*. 2021; Vohra *et al*. 2021), and image preprocessing (He *et al*. 2019; Mo and Chen 2021). By such measures, extraction and separation of target feature can be achieved. The HSV color space shows unique advantages in stained image analysis because it simulates the human visual perception characteristics of hue, saturation, and value. For example, Herzberg-stained hemp pulp fibers appear burgundy in the HSV space, while wood pulp fibers show a blue tone, and accurate segmentation can be achieved through threshold setting. Compared with the traditional RGB color space (Liu *et al*. 2023; Tadahiro *et al*. 2024), the HSV space is more robust against variations in staining concentration and uneven lighting, and the analysis results better align with subjective perception. Although MATLAB's image processing toolbox has already been used for fiber diameter measurement (Murphy *et al*. 2020; Ruan *et al*. 2020) and deformation analysis (Belyaev *et al*. 2010), there is still a lack of systematic studies on multicomponent quantitative analysis in mixed pulp systems. To address the efficiency limitations of traditional methods, this study innovatively introduced digital image recognition technology and built an HSV color space model using MATLAB. The preprocessing parameters of the stained fiber images were optimized, and the fiber color features were extracted using threshold segmentation. The experiment consisted of 4 sets of two-component and 2 sets of three-component mixed pulps. By combining pixel value visualization and fiber mass factor, rapid analysis of fiber mass ratios was achieved. The results showed that this method had no significant difference in accuracy compared with the ImageJ analysis method, but the time required for the determination was significantly shortened. This technique was further applied to seven types of commercial cigarette paper to verify its feasibility in practical applications. This study integrates staining techniques with image processing technology, thereby overcoming the subjectivity of manual interpretation and providing an efficient analytical method for selecting raw materials and optimizing the production process of cigarette paper, demonstrating industrial application potential.

EXPERIMENTAL

Materials

Hardwood pulp: Bleached kraft eucalyptus pulp, brand *Carabin (Eucalyptus)*, origin: Brazil. Softwood pulp: Bleached kraft pine pulp, brand *Forest (Picea asperata Mast)*, origin: Sweden. Hemp pulp: Flax (*Linum usitatissimum L*), imported hemp pulp. All the above pulp samples were provided by Zhejiang Minfeng Special Paper Co., Ltd. (Jiaxing, China).

Based on current market sales and production processes, seven types of commercial cigarette paper samples were selected. Detailed sample information is shown in Table 1. Sample S1 was provided by Hengfeng Paper Co., Ltd. Samples S2 and S3 were both provided by Modipap (France). Sample S4 was provided by Zhejiang Huafeng Paper Group Co., Ltd. Sample S5 was provided by China Tobacco Modipap (Jiangmen) Paper

Co., Ltd., and samples S6 and S7 were also provided by China Tobacco Modipap (Jiangmen) Paper Co., Ltd.

Zinc chloride ($ZnCl_2$, 98%) was purchased from Shanghai Aladdin Biochemical Technology Co., Ltd.; potassium iodide (KI), iodine (I_2), and calcium chloride ($CaCl_2$, 97%) were purchased from Nanjing Chemical Reagent Co., Ltd.; aluminum chloride ($AlCl_3$, 97%) was purchased from Sinopharm Chemical Reagent Co., Ltd. All reagents were of analytical grade.

IMT-SJ01 standard fiber disintegrator from Intane Precision Instruments Co., Ltd.; BX41 optical microscope from Olympus (China) Co., Ltd.; and Morfi Compact fiber quality analyzer was from Techpap (France) were used for analysis.

Table 1. Specific Information of the Seven Commercial Cigarette Paper Samples

Sample ID	Manufacturer
S1	Hengfeng Paper Industry Co., Ltd.
S2	MD Papiers (France) China Tobacco Modipap (Jiangmen) Co., Ltd.
S3	
S4	Zhejiang Huafeng Paper Group Co., Ltd.
S5	China Tobacco Modipap (Jiangmen) Co., Ltd.
S6	China Tobacco Modipap (Jiangmen) Co., Ltd.
S7	China Tobacco Modipap (Jiangmen) Co., Ltd.

Preparation of Herzberg Staining Solution

The standard Herzberg staining solution was prepared following GB/T 4688-2020 (National Technical Committee for Standardization of the Paper Industry, 2020). The procedure says to mix 15 mL of Solution A (saturated $ZnCl_2$ solution prepared at room temperature) and 5 mL of Solution B (prepared by completely dissolving 2.1 g of potassium iodide and 0.1 g of iodine in 5 mL of water). The mixture was left in the dark for more than 6 hours until all precipitates have settled. Then, the upper clear solution is poured into a brown dropper bottle and a small piece of iodine (I_2) is added to complete the preparation.

Preparation of Graff "C" Standard Staining Solution

The standard Graff "C" staining solution was prepared in accordance with GB/T 4688-2020 standard (National Technical Committee for Standardization of the Paper Industry, 2020). About 20 mL of Solution A (40 g of aluminum chloride hexahydrate dissolved in 100 mL of water), 10 mL of Solution B (100 g of calcium chloride dissolved in 150 mL of water), 10 mL of Solution C (100 g of dry zinc chloride dissolved in 50 mL of warm water), and 12.5 mL of Solution D (0.9 g of potassium iodide and 0.65 g of iodine dissolved in 50 mL of distilled water) were mixed. The mixture was left in the dark for 12 to 24 h until complete precipitation occurs. The supernatant was gently poured into a brown dropper bottle, and a small piece of iodine (I_2) was added to complete the preparation.

Preparation of Mixed Pulps and Samples

To determine the water content, about 0.1 g of oven-dried fiber sample or commercial paper fiber sample was weighed according to different proportions. The fibers

were soaked in 100 mL of deionized water and stirred with a glass rod until the fibers were dispersed to form a 0.1% fiber suspension. About 1 to 2 drops of the fiber suspension were placed in the center of a glass slide and dried in a 60 °C oven. After cooling, about 1 to 2 drops of staining solution were added. A coverslip was pressed using tweezers on one side of it at a 45° angle. Then, it was slowly lowered to avoid bubbles. A filter paper was used to absorb excess staining solution around the coverslip. Once the sample was confirmed to be ready, it was observed immediately. Separate stained microscope slides were prepared for Herzberg and Graff "C" staining solutions. The stained slides were observed under an optical microscope. The digital images were acquired using the integrated digital imaging system of the Olympus BX41 optical microscope. The raw data were delivered in a standard 24-bit RGB color format. In this format, each image was stored as a 3D matrix in MATLAB, where each pixel is represented by an RGB triple. Each channel (Red, Green, Blue) uses 8 bits, with intensity values ranging from 0 to 255. The resolution for image acquisition was set to 2048 × 1536 pixels. Each pixel in the digital image is associated with its own unique RGB value. No spatial averaging or downsampling was performed during acquisition or prior to the HSV conversion to ensure that the fine morphology and edges of the stained fibers were preserved for accurate segmentation. The analysis was performed using 40× and 100× objective lenses. At 40× magnification, the corresponding physical field of view is approximately 0.65 mm × 0.48 mm. For each sample, ten representative images were selected for analysis to ensure statistical representativeness. Each observation experiment was repeated more than three times from sample preparation.

HSV Color Space Conversion and Image Preprocessing

In this study, MATLAB R2023b (Meiswok Software Co., Ltd.) software was used for color space selection and conversion. The RGB color space was converted to the HSV color space to facilitate more stable color segmentation. The primary advantage of the HSV color space is its ability to separate the hue channel from the intensity and saturation channels, thereby providing better value stability compared to the RGB color space. This rationale was central to the research design, as it ensures that the target fiber colors remain identifiable even under slight variations in lighting conditions during image acquisition. Fiber images stained with Herzberg and Graff "C" staining solutions were processed separately to ensure optimal image quality. To identify the optimal enhancement conditions, the saturation gain factors were set at 1.0, 1.5, and 2.0 for Herzberg staining, and 1.0, 2.0, and 3.0 for Graff "C" staining, while brightness enhancement factors were tested at 1.0, 1.1, and 1.2 respectively. These specific candidate values were chosen based on preliminary experimental observations, aiming to explore the boundary between effectively enhancing color contrast for segmentation and avoiding unnatural artifacts or overexposure that could lead to information loss. For images stained with Graff "C" solution, the saturation gain factor was set to 1.0, 2.0, and 3.0, and the brightness gain factor was set to 1.0, 1.1, and 1.2. The processed images were compared to determine the best optimization parameters. The relevant program code in MATLAB is shown as follows:

```
hsv_img = rgb2hsv(img);
increase_saturation_factor = 1.5;
hsv_img(:,:,2) = hsv_img(:,:,2) * increase_saturation_factor;
hsv_img(hsv_img > 1) = 1;
increase_value_factor = 1.1;
hsv_img(:,:,3) = hsv_img(:,:,3) * increase_value_factor.
```

Color Threshold Segmentation Based on *H*, *S*, and *V*

The RGB color space was converted to the HSV color space, which is conceptualized as a hexcone model. Based on the optical characteristics of stained fibers and visual perception principles, threshold ranges were manually set to specify the maximum and minimum values of desired hue (*H*), saturation (*S*), and value (*V*). To identify the optimal enhancement conditions, saturation gain factors were specifically set at 1.0, 1.5, and 2.0, while brightness enhancement factors were fixed at 1.0, 1.1, and 1.2. These values were chosen to create a controlled gradient for testing, aiming to find the precise balance where color contrast is sufficiently enhanced for segmentation without introducing overexposure or "color distortion" that could compromise fiber morphology. The hue (*H*) range was determined based on a standard color chart and the actual values measured from microscopic images. Next, binarization was performed, and a mask was constructed and applied to the original image to facilitate segmentation, enabling the extraction and separation of different types of fibers, which were then visualized based on pixel values. After HSV color space converting, fiber morphology and thickness affect color feature extraction. For example, curled or branched fibers can lead to uneven staining and localized color variations. The naturally crimped structure of jute pulp fibers may cause different areas of the same fiber to show hue differences in the HSV space, increasing the likelihood of misclassification during segmentation. Over-segmentation or omission will be caused if apply uniform threshold. Additionally, fiber overlap can cause HSV values in overlapping regions to exhibit mixed effects, where hues may shift, forming an intermediate color characteristic between the two, which can lead to incorrect classification during threshold segmentation as an independent fiber type.

Fiber Coarseness and Quality Factor Analysis Based on FQA

A 40 mg of absolute-dried sample of mixed pulp was placed in a 50 mL test tube, mixed with one-third deionized water. A few glass beads were added to disperse the pulp fully into single fibers. Then, the sample was transferred to the sample beaker of the fiber quality analyzer and mixed with deionized water to bring the total volume to 1 L. The fiber quality analyzer was used to measure the mass parameters. The coarseness of the mixed or commercial paper fibers was recorded, and the corresponding quality factor was calculated using the following formula,

$$f_{\mathrm{x}}=\frac{C_{\mathrm{x}}}{0.180} \quad (1)$$

where f_{x} is mass factor of blended pulp fibers and C_{x} is coarseness of blended pulp fibers (mg/m).

Fiber Composition Analysis

After separating different types of fibers, the number of pixels of each fiber type stained with either Herzberg or Graff "C" staining agents was measured using MATLAB R2023b, and the total number of fiber pixels was also determined. Combined with fiber width and quality factor, the proportion of each fiber type in the mixed pulp was calculated using Eqs. 2 and 3.

$$X_{\mathrm{n}}=\frac{f_{\mathrm{n}} N_{\mathrm{n}}}{\bar{f} N_{\mathrm{t}}} \times 100\% \quad (2)$$

$$\mathrm{N_n}=\frac{\mathrm{M_n}}{\mathrm{W_n}} \quad (3)$$

In Eqs. 2 and 3, X_n is mass ratio (%) of a specific fiber type; f_n is mass factor of a specific fiber type; N_n is total length (mm) of a specific fiber type; $\bar{f}$ is average mass factor of blended fibers; N_t is total length (mm) of all fiber types; M_n is pixel area of a specific fiber; and W_n is width (μm) of a specific fiber.

RESULTS AND DISCUSSION

Determination of Image Preprocessing Conditions

In digital image processing, saturation gain factors typically range from 1.0 to 2.0 to achieve optimal contrast enhancement while preserving natural color boundaries (Gonzalez and Woods 2018; Vyas *et al*. 2018). It is well-documented that excessively high saturation enhancement factors can lead to significant color distortion, such as the loss of fine structural details and the occurrence of "clipping" artifacts, which would compromise the reliability of subsequent fiber segmentation (Tadahiro *et al.* 2024).

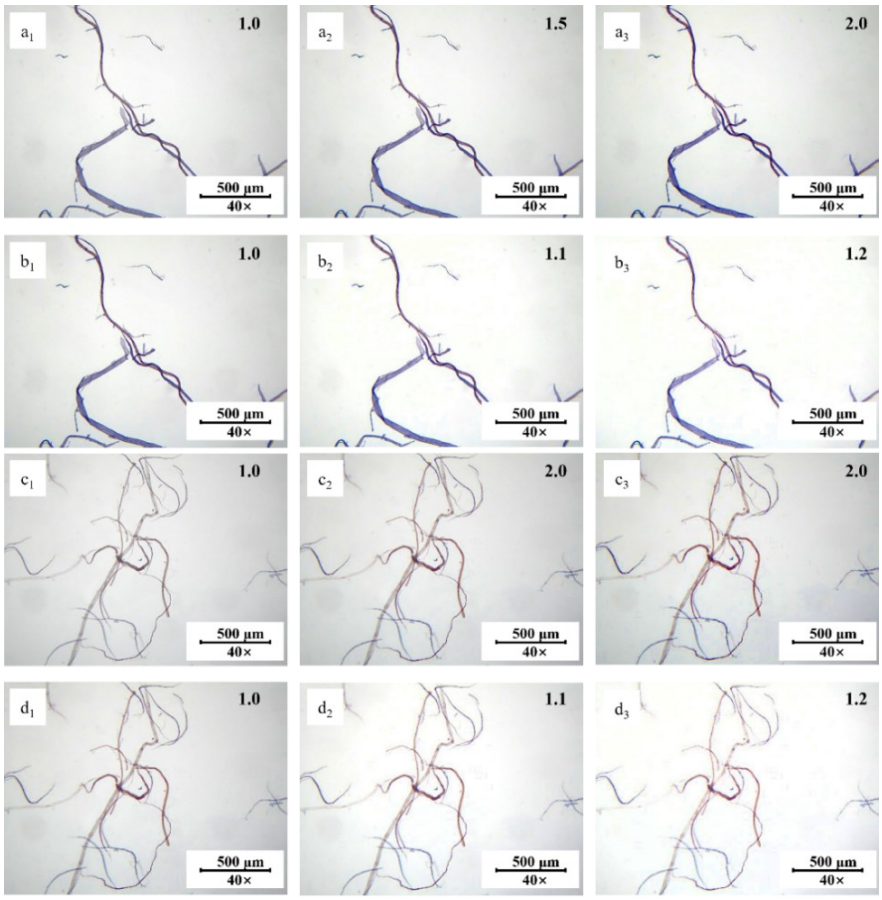

Fig. 1. Micrographs of a three-component fiber mixture (softwood pulp: hardwood pulp: hemp pulp = 5:3:2) under an optical microscope: (a) images of the mixture stained with Herzberg reagent; (b) images of the mixture stained with Graff "C" reagent. The pretreatment conditions of the images after dyeing with two kinds of dyes were established: a_1, a_2, and a_3 were images with constant brightness and saturation gain factors of 1.0, 1.5, and 2.0 after Herzberg staining, respectively; b_1, b_2, and b_3 were images with the saturation gain fixed at 1.5 and brightness gain factors of 1.0, 1.1, and 1.2, respectively; c_1, c_2, and c_3 were images stained with Graff "C" obtained with saturation gain factors of 1.0, 2.0, and 3.0, respectively; and d_1, d_2, and d_3 were images obtained with a saturation gain factor of 2.0 and brightness gain factors of 1.0, 1.1, and 1.2, respectively.

Excessively high saturation gain can lead to color distortion or unnatural appearance of the image. As shown in Fig. 1, keeping brightness constant, saturation gain factors were set to 1.0 (a1), 1.5 (a2), and 2.0 (a3). Results showed that when the saturation gain factor was 1.5, the color improved significantly, and the image showed no distortion. When the saturation gain factor was 2.0, the image showed obvious color distortion and unnatural phenomena; thus, 1.5 was identified as the optimal saturation gain value. Furthermore, the saturation gain factor was kept at 1.5, while the brightness gain factors were set to 1.0 (b1), 1.1 (b2), and 1.2 (b3). It was found that, when the brightness gain factor was 1.1, the image brightness improved effectively without overexposure problems. When the brightness gain was 1.2, the highlight areas of bright parts of the image showed obvious detail losses. For images stained with Graff "C", saturation gain factors were set to 1.0 (c1), 2.0 (c2), and 3.0 (c3). The results showed that when the saturation gain factor was 2.0, the optimization of color vividness was the most significant. When the saturation gain factor was 3.0, the image exhibited color distortion. Based on this, brightness gain factors were set to 1.0 (d1), 1.1 (d2), and 1.2 (d3), and founded that when the brightness gain factor is 1.1, best color presentation occurred, and at 1.2, detail losses occurred at the highlight areas, thus 1.1 was confirmed as the optimal brightness gain factor.

Analysis of Mixed Pulp Fiber Composition through Staining Method Combined with Image Recognition Method

Two-component pulp mixture of softwood and hardwood pulps

A total of 0.1 g of absolute-dried pulp (with softwood-to-hardwood ratios of 2:3 and 3:2) was weighed and used to prepare a 0.01% fiber suspension. Two drops were pipetted onto the center of a glass slide and dried in an oven at 60 °C. The samples were stained with Herzberg and Graff "C" dyes diluted to 90% of their original concentration for 20 s and 30 s, respectively. Prepared into microscopic slides after dyeing, and the images were captured using an optical microscope.

Since the samples contained both softwood and hardwood pulps, ten images stained with Graff "C" dye were selected from each experimental group for image preprocessing (Fig. 2).

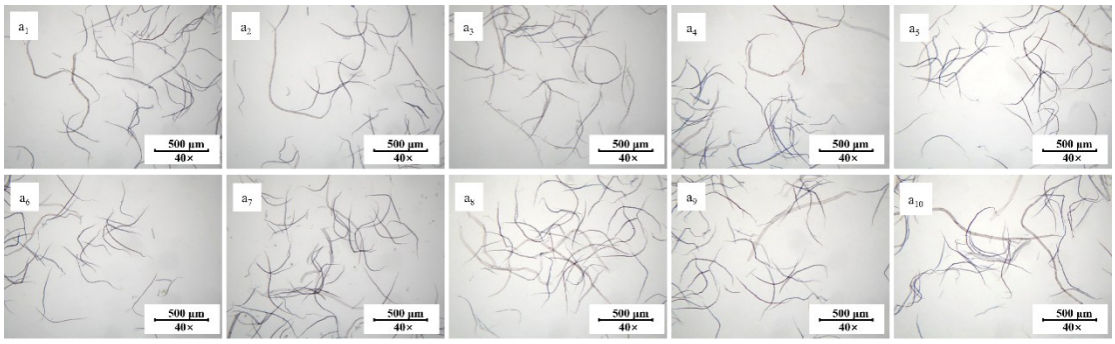

Fig. 2. Image of two-component pulp (softwood pulp: broadleaf pulp = 2:3) under an optical microscope. Group a is the microscope images of Softwood (softwood pulp): Hardwood (broadleaf pulp) = 2:3 pulp stained by Helzberg and Graff "C", when the saturation factor is set to 2.0 and the brightness gain factor is 1.5.

For the first experimental group (softwood:hardwood = 2:3), the fiber images underwent preprocessing with the saturation gain factor set to 2.0 and the brightness gain factor set to 1.5. The images were then converted to the HSV color space, and the color

thresholding method was used to extract all types of fibers as well as specifically the blue-gray fibers (hardwood pulp fibers), as shown in Fig. 3. Subsequently, the number of pixels corresponding to all fibers and to hardwood fibers was counted to analyze the mass ratio of hardwood to total fibers. The fiber analysis for the second experimental group (softwood:hardwood = 3:2) followed the identical procedure described above. The resulting images showing the extracted fibers for this group are presented in Figs. 4 and 5.

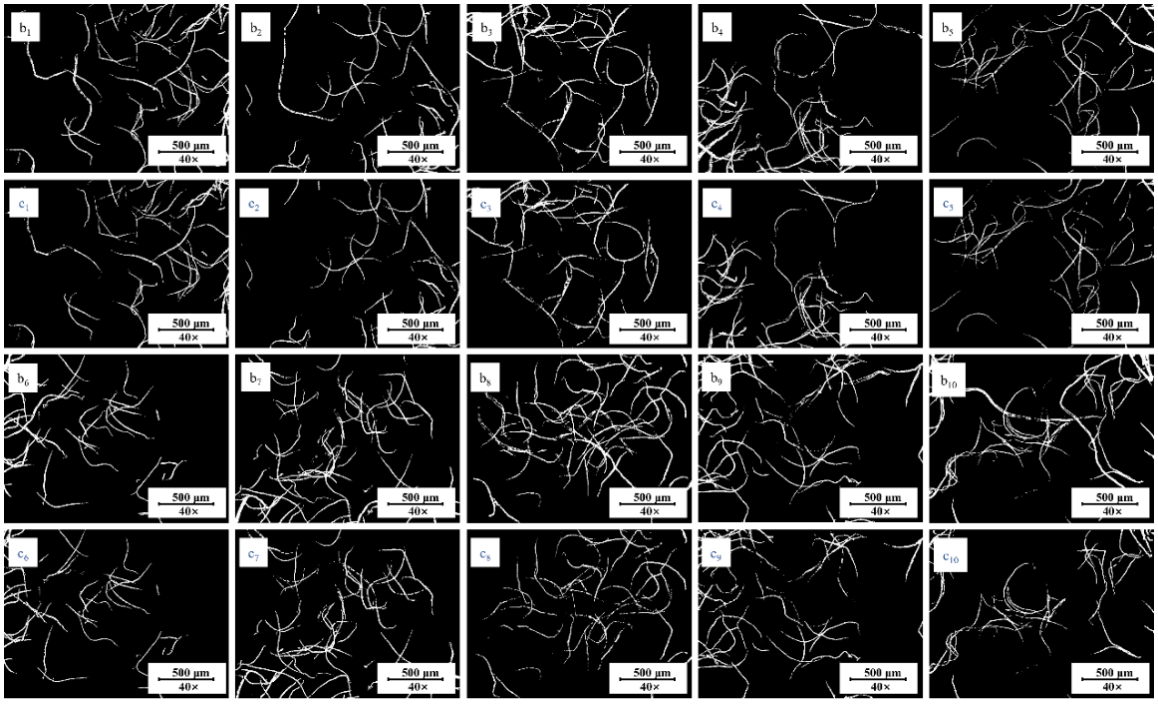

Fig. 3. Images of the fibers after separation and extraction of two-component pulp (softwood pulp: broadleaf pulp = 2:3). Here group b is the picture of extracting all fibers, group, and c is the picture of extracting broadleaf fibers.

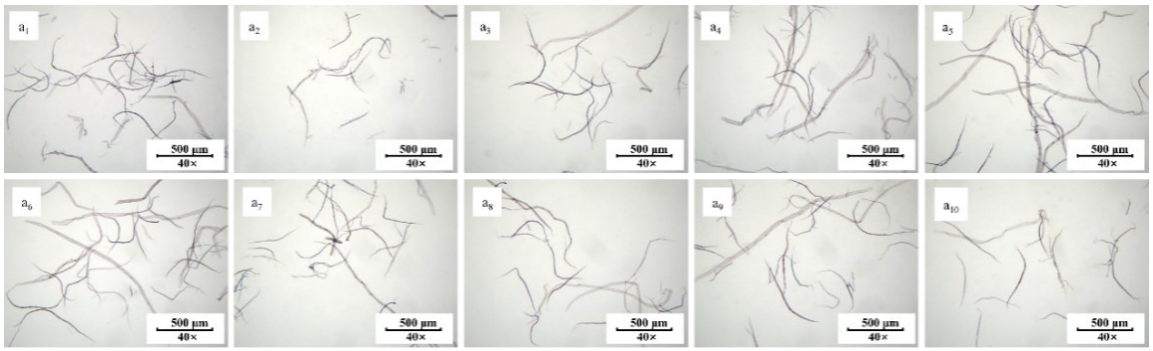

Fig. 4. Image of two-component pulp (softwood pulp: broadleaf pulp = 3:2) under an optical microscope. Group a is the microscope images of Softwood (softwood pulp): Hardwood (broadleaf pulp) = 3:2 pulp stained by Helzberg and Graff "C", when the saturation factor is set to 2.0 and the brightness gain factor is 1.5.

Following the method described in experimental section, the fiber coarseness and fiber width of both mixed pulp samples were measured using a fiber quality analyzer. The corresponding mixed fiber quality factors were calculated. The mass proportion of each

fiber type was determined separately, combined with the pixel counts. The results are shown in Table 2.

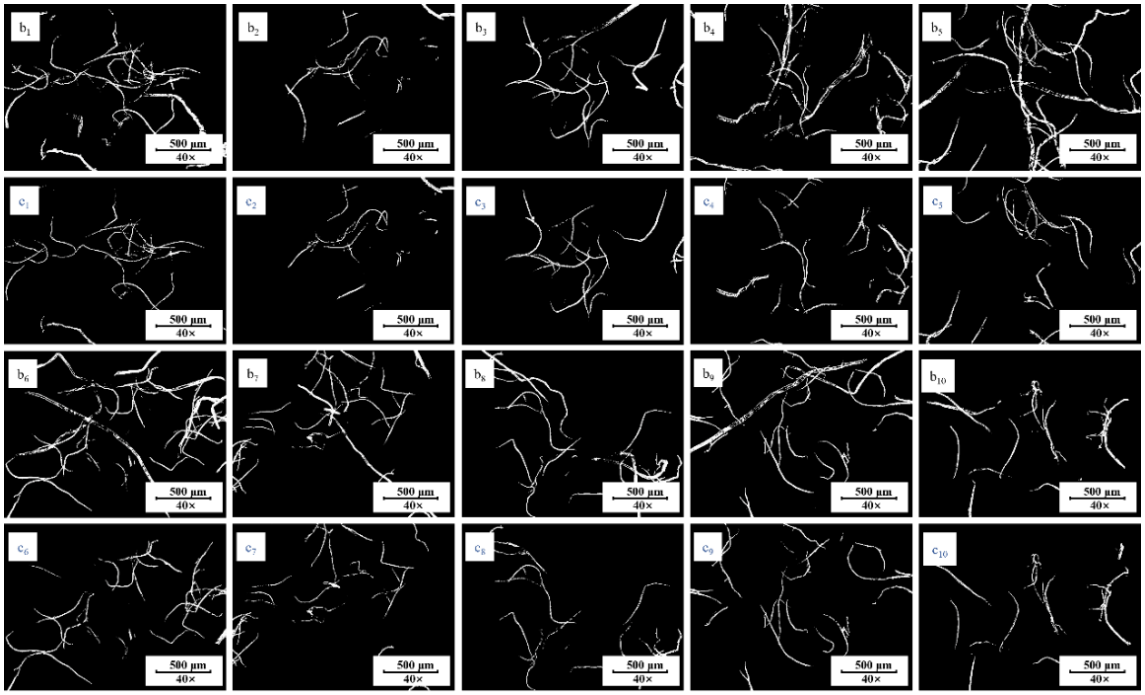

Fig. 5. Images of the fibers after separation and extraction of two-component pulp (softwood pulp: broadleaf pulp = 3: 2). Here group b is the picture of extracting all fibers, group and c is the picture of extracting broadleaf fibers.

Table 2. Quantitative Accuracy Analysis of Two-Component Mixed Pulp Fiber

	Actual Mass Ratio (%)		Analyzed Mass Ratio (%)		Relative Error (%)		Average Error (%)	Accuracy (%)
	Softwood Pulp	Hemp Fiber	Softwood Pulp	Hemp Fiber Pulp	Softwood Pulp	Hemp Fiber Pulp		
1	40.0	60.0	46.8	53.2	16.9	11.3	14.1	85.9
2	60.0	40.0	65.7	34.3	9.5	14.3	11.9	88.1

Two-component pulp mixture (softwood and hemp pulps)

A total of 0.1 g of absolute-dried pulp (with softwood-to-Hemp pulp ratios of 2:3 and 72.7:27.3) was weighed and used to prepare a 0.01% fiber suspension. Two drops were pipetted onto the center of a glass slide and dried in an oven at 60 °C. The samples were stained with Herzberg and Graff "C" dyes diluted to 90% of their original concentration for 20 s and 30 s, respectively. Prepared into microscopic slides after dyeing, and the images were captured using an optical microscope. Since the samples contained only softwood and hemp pulp, only the fiber images after being stained with Herzberg dye need to be analyzed. For the first experimental group (softwood pulp: hemp fiber pulp = 2:3), ten images stained with Herzberg dye were selected for fiber analysis (Fig. 6). In MATLAB, the acquired fiber images underwent preprocessing with the saturation gain factor set to 2.0 and the brightness gain factor set to 1.5. The images were then converted to the HSV color space. Using the color thresholding method, all types of fibers and

specifically the blue fibers (softwood pulp fibers) were extracted, as shown in Fig. 7, followed by binarization. Subsequently, the number of pixels corresponding to all fibers and to the Hemp fibers was counted to analyze the mass ratio of hemp fibers to total fibers. The fiber analysis for the second experimental group (softwood pulp: hardwood pulp = 3:2) followed the identical procedure described above. The resulting extracted fiber images for this group are presented in Figs. 8 and 9.

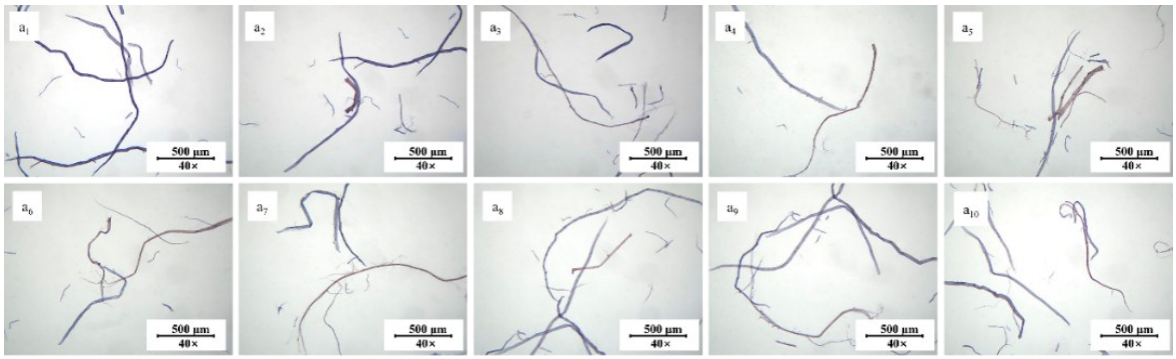

Fig. 6. Image of two-component slurry (softwood pulp: hemp pulp = 2: 3) taken under an optical microscope. Group a is the microscope images of softwood: hemp = 2:3 pulp stained by Helzberg and Graff "C", when the saturation factor is set to 2.0 and the brightness gain factor is 1.5.

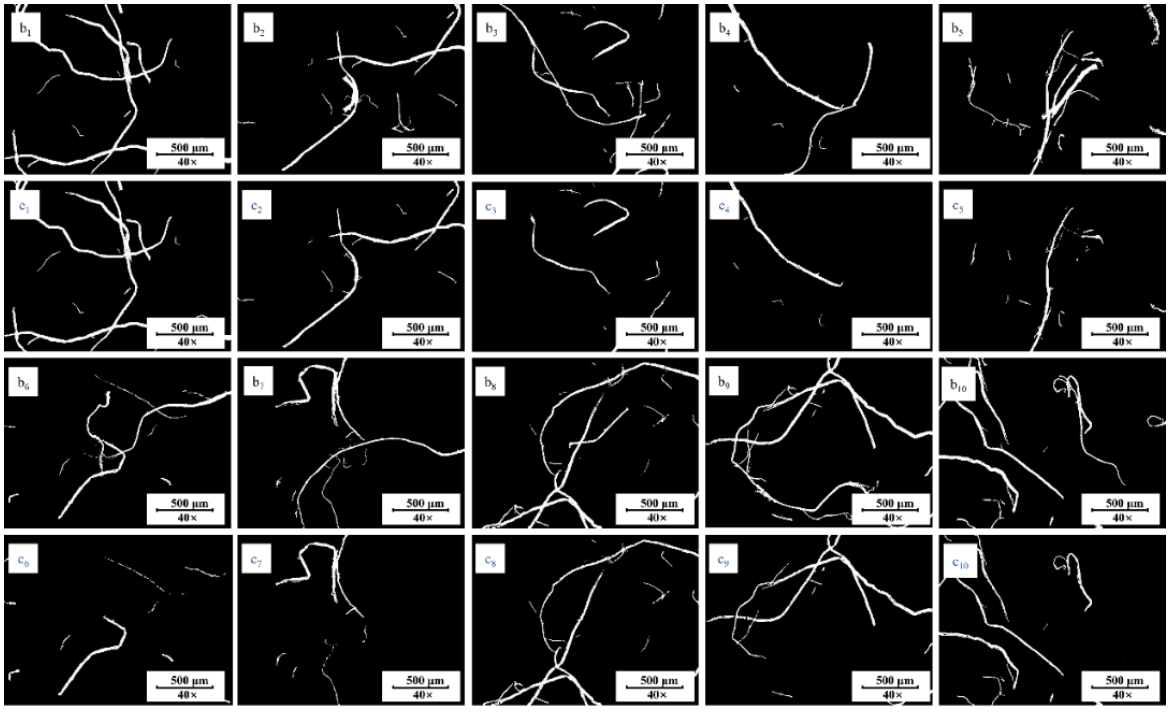

Fig. 7. Images of the fibers after separation and extraction of two-component pulp (softwood pulp: hemp pulp = 3: 2). Here group b is the picture of extracting all fibers, and group c is the picture of separating hemp pulp fibers.

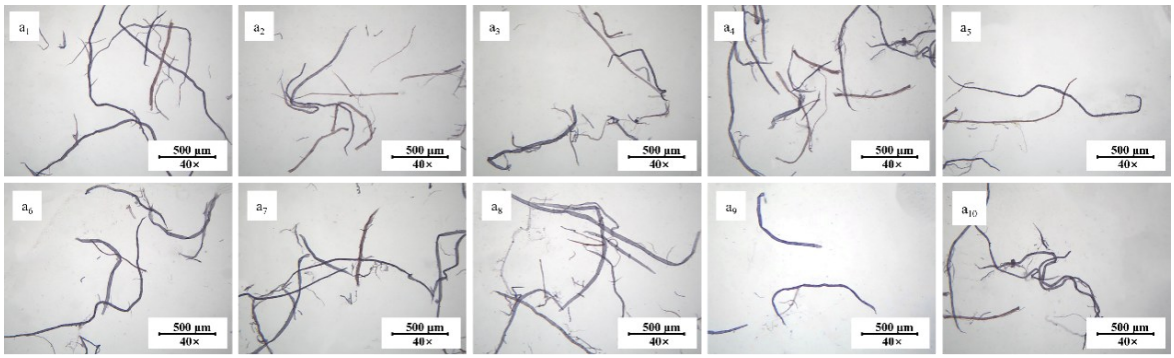

Fig. 8. Image of two-component slurry (softwood: hemp = 72.7:27.3) taken under an optical microscope. Group a is the microscope images of softwood: hemp = 72.7:27.3 pulp stained by Helzberg and Graff "C", when the saturation factor is set to 2.0 and the brightness gain factor is 1.5.

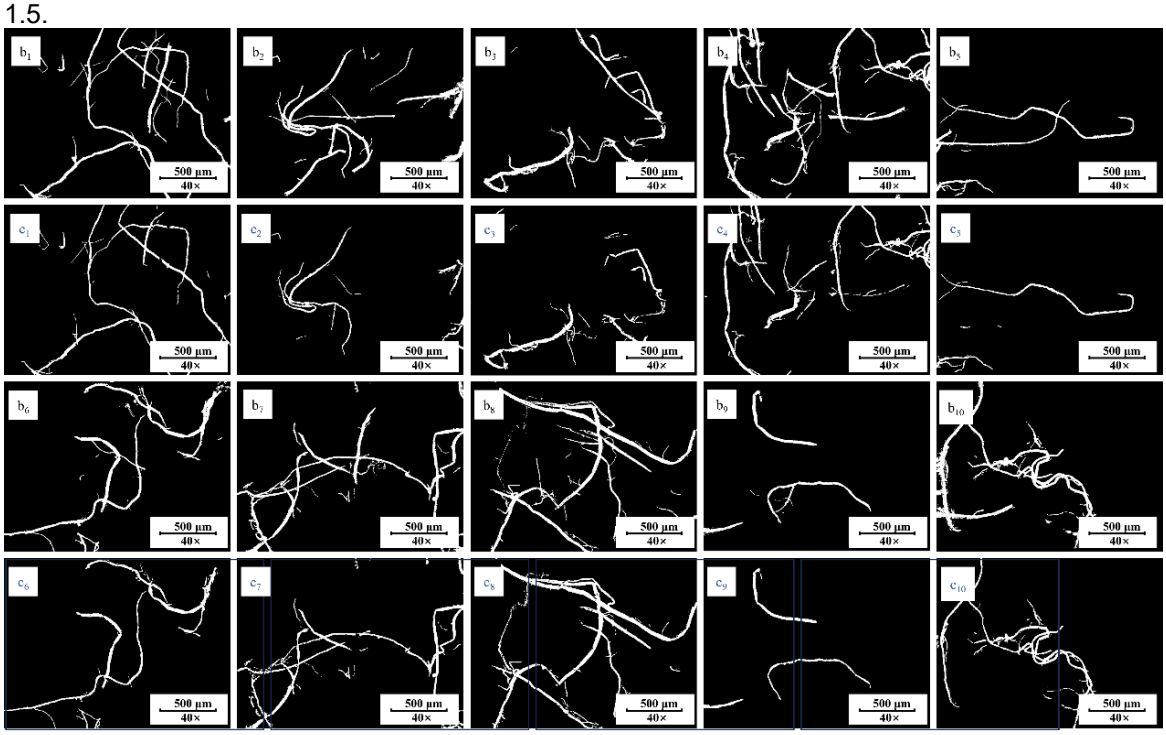

Fig. 9. Images of the fibers after separation and extraction of two-component pulp (softwood pulp: hemp pulp = 72.7:27.3). Here group b is the picture of extracting all fibers, group and c is the picture of separating hemp pulp fibers.

Following the method described before, the fiber coarseness and fiber width of both mixed pulp samples were measured using a fiber quality analyzer. The corresponding mixed fiber quality factors were calculated. The mass proportion of each fiber type was determined separately, combined with the pixel counts. The results are shown in Table 3.

Table 3. Quantitative Accuracy Analysis of Two-Component Mixed Pulp Fiber

	Actual Mass Ratio (%)		Analyzed Mass Ratio (%)		Relative Error (%)		Actual Mass Ratio (%)	Analyzed Mass Ratio (%)
	Softwood Pulp	Hemp Fiber Pulp	Softwood Pulp	Softwood Pulp	Hemp Fiber Pulp	Softwood Pulp		
1	40.0	60.0	37.5	62.5	6.2	4.1	5.1	94.9
2	72.7	27.3	73.4	26.5	1.1	2.8	1.9	98.1

Three-component pulp mixture (softwood, hardwood, and hemp pulps)

A total of 0.1 g of absolute-dried pulp (with softwood: hardwood: hemp ratios of 5:3:2 and 5:2:3) was weighed and prepared a 0.01% fiber suspension. Two drops were pipetted onto the center of a glass slide and dried in an oven at 60 °C. The samples were stained with Herzberg and Graff "C" dyes diluted to 90% of their original concentration for 20 s and 30 s, respectively. Prepared into microscopic slides after dying, and the images were captured using an optical microscope.

For the first experimental group (softwood pulp : hemp fiber pulp = 2:3), ten stained images were selected for analysis as shown in Fig. 10.

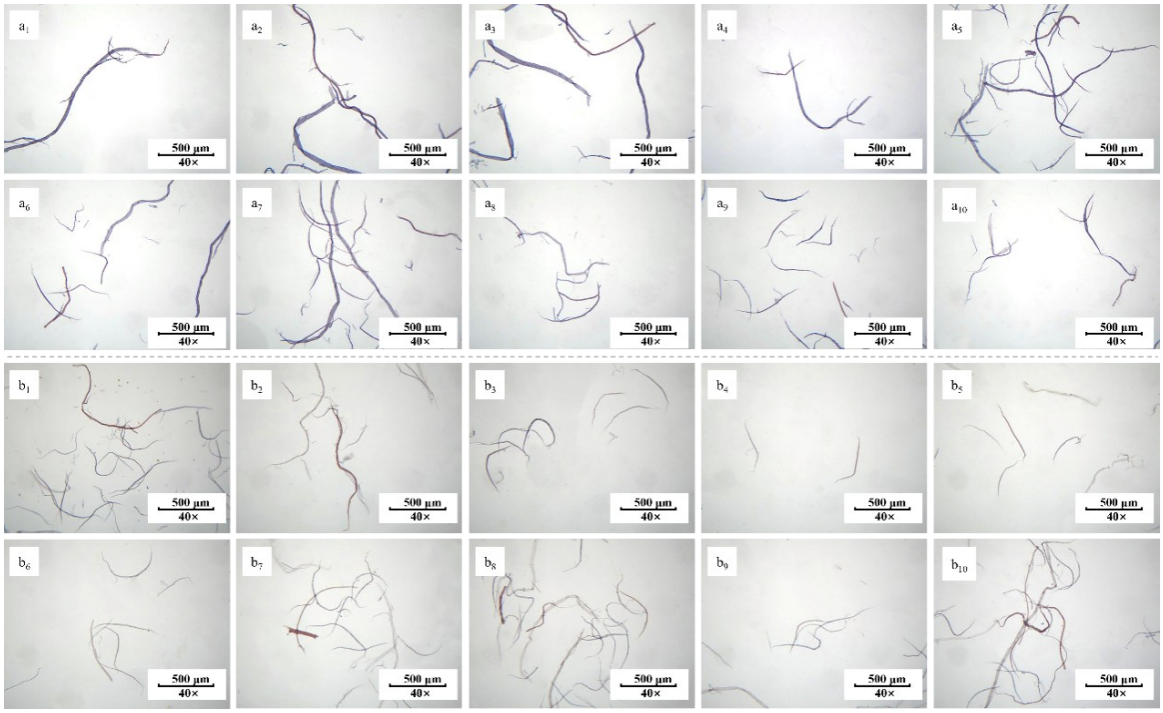

Fig. 10. Image of three component pulp mixture (softwood pulp: broadleaf pulp: hemp pulp = 5:3:2) taken under an optical microscope. Group a is the microscope image of the pulp of softwood pulp: broadleaf pulp: hemp pulp = 5:3:2 after Hertzberg staining, when the saturation factor is set to 2.0 and the brightness gain factor is 1.5.Group b is the microscope image of softwood pulp: broadleaf pulp: hemp pulp = 5:3:2 and then stained with Graff "c", when the saturation factor is set to 2.0 and the brightness gain factor is 1.5.

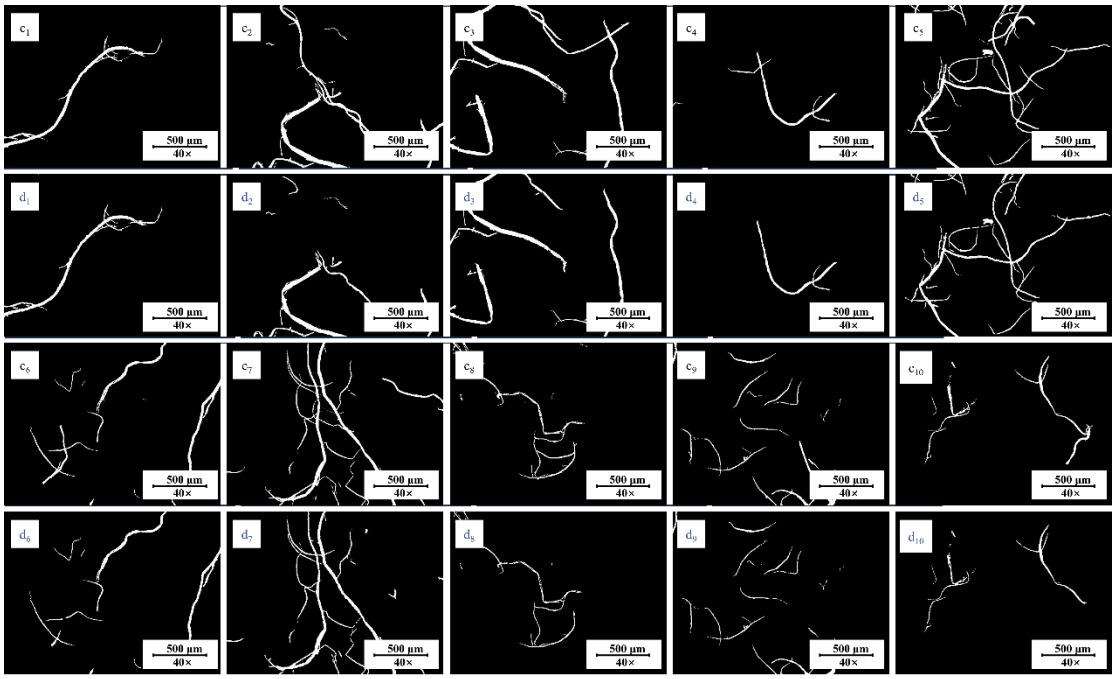

Fig. 11. Images of the fibers after separation and extraction of three component pulp (softwood pulp:broadleaf pulp:hemp pulp = 5:3:2) after dyeing by Herzberg. Here group c is the picture of extracting all fibers, and group d is the picture of separating hemp pulp fibers.

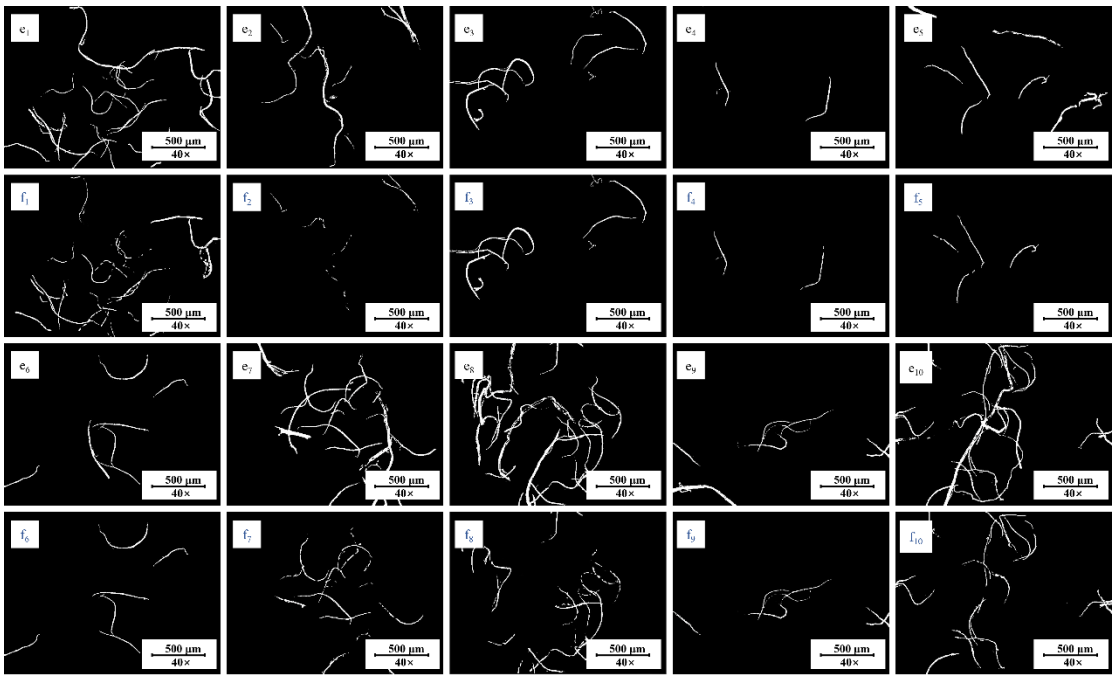

Fig. 12. Images of the fibers after separation and extraction of three component pulp (softwood pulp: broadleaf pulp: hemp pulp = 5:3:2) after dyeing by Graff"C". Here group e is the picture of extracting all fibers, and group f is the picture of extracting broadleaf fibers.

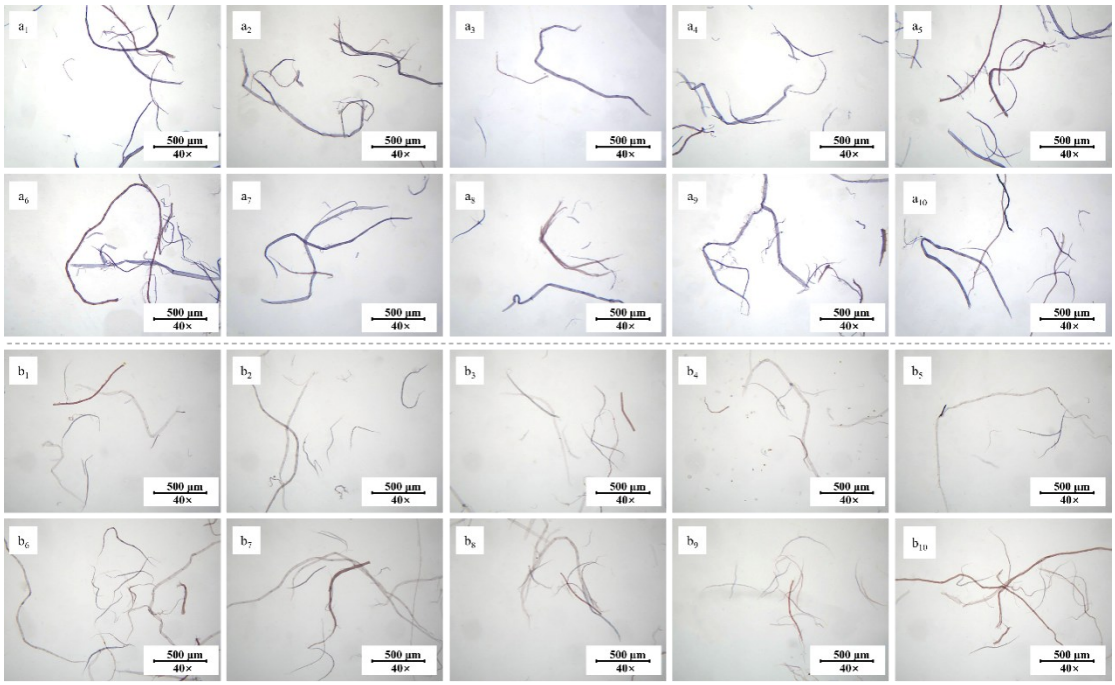

Fig. 13. Image of three component pulp (softwood pulp: broadleaf pulp: hemp pulp = 5:2:3) taken under an optical microscope. Group a is the microscope image of the pulp of softwood pulp: broadleaf pulp: hemp pulp = 5:2:3 after Hertzberg staining, when the saturation factor is set to 2.0 and the brightness gain factor is 1.5.Group b is the microscope image of softwood pulp: broadleaf pulp: hemp pulp = 5:2:3 and then stained with Graff "C", when the saturation factor is set to 2.0 and the brightness gain factor is 1.5.

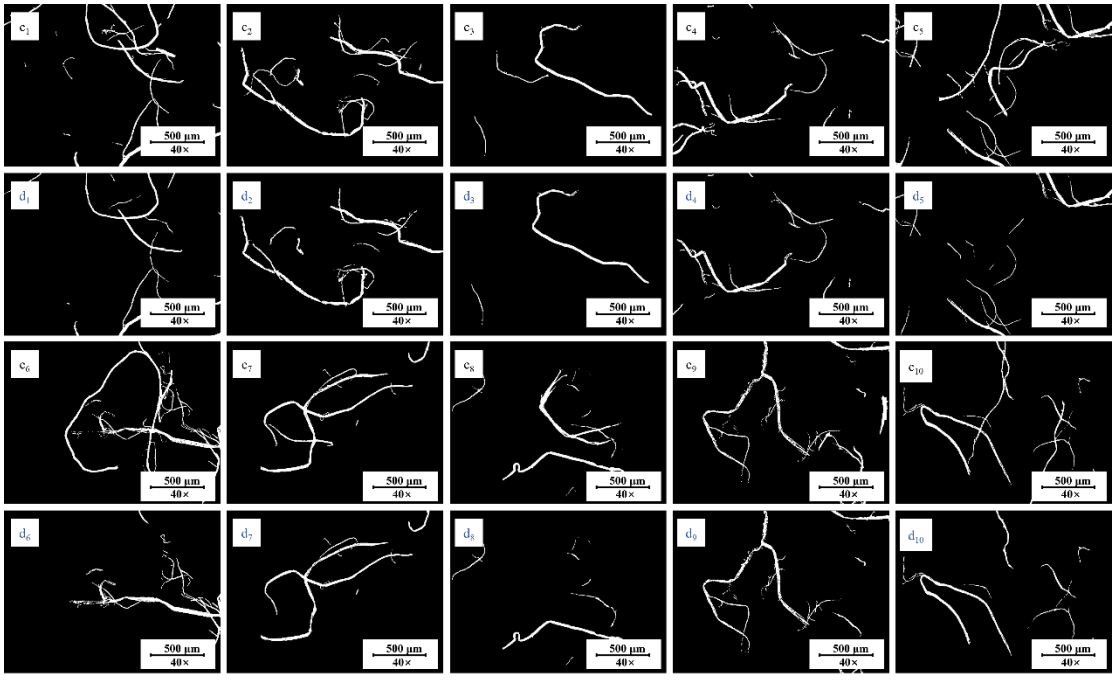

Fig. 14. Images of the fibers after separation and extraction of three component pulp (softwood pulp:broadleaf pulp:hemp pulp = 5:2:3) after dyeing by Herzberg. Here group c is the picture of extracting all fibers, and group d is the picture of separating hemp pulp fibers.

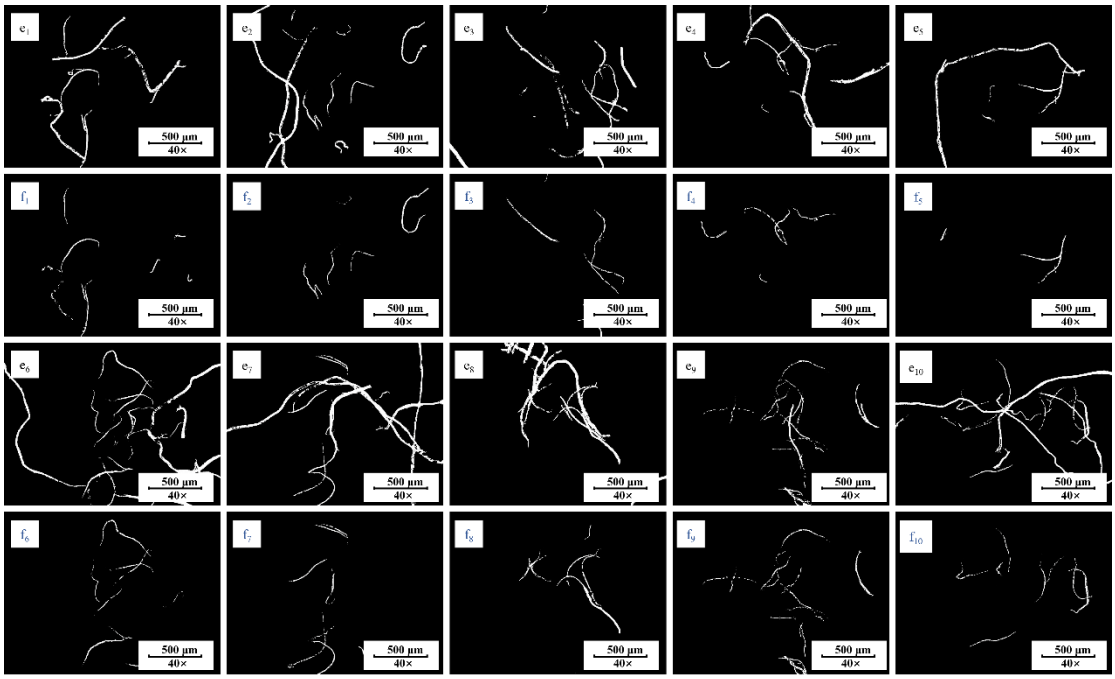

Fig. 15. Images of the fibers after separation and extraction of three component pulp (softwood pulp: broadleaf pulp: hemp pulp = 5:2:3). Here group e is the picture of extracting all fibers, and group f is the picture of extracting broadleaf fibers.

Following preprocessing, the color thresholding method was applied to extract all fiber types and specifically the blue fibers (wood pulp fibers, primarily softwood) from Herzberg stained images, and all fiber types along with the blue-gray fibers (hardwood fibers) from Graff "C" stained images, with the resulting extracted fiber images presented in Figs. 11 and 12, respectively. Subsequently, pixel counts for different fiber types were quantified to calculate relevant mass ratios. The second experimental group with a softwood pulp to hardwood pulp ratio of 3:2 was similarly processed using identical staining and analysis procedures, yielding extracted fiber images shown in Figs. 13 to 15.

Following the method described before, the fiber coarseness and fiber width of both mixed pulp samples were measured using a fiber quality analyzer. The corresponding mixed fiber quality factors were calculated. The mass proportion of each fiber type was determined separately, combined with the pixel counts. The results are shown in Table 4.

Table 4. Quantitative Accuracy Analysis of Three-Component Mixed Pulp Fiber

Actual Mass Ratio (%)			Analyzed Mass Ratio (%)			Relative Error (%)			Actual Mass Ratio (%)	Analyzed Mass Ratio (%)
Softwood Pulp	Hemp Fiber Pulp	Softwood Pulp	Softwood Pulp	Hemp Fiber Pulp	Softwood Pulp	Softwood Pulp	Hemp Fiber Pulp	Softwood Pulp		
50.0	30.0	20.0	49.1	28.4	22.6	1.9	5.5	12.9	6.8	93.3
50.0	20.0	30.0	49.9	17.6	32.5	0.2	12.1	8.4	6.9	93.1

Analysis of Commercial Cigarette Paper Fiber Composition through Staining Method Combined with Image Recognition Method

The commercial cigarette paper samples S1 to S7 described before were prepared into 0.01% fiber suspensions and stained with two types of dyes separately.

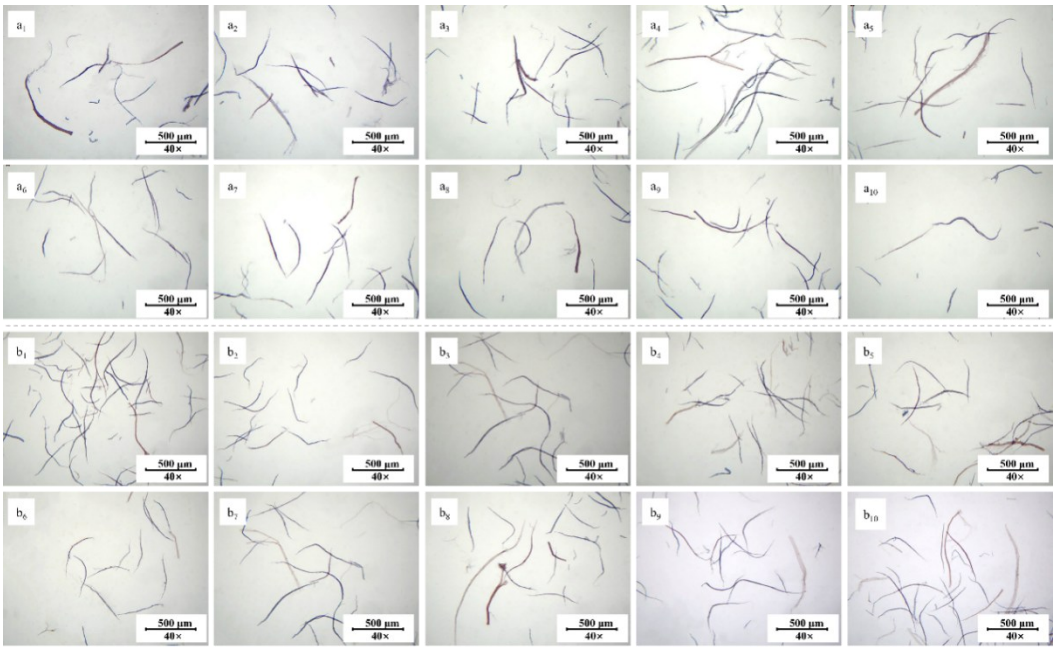

Fig. 16. Image of S1 cigarette paper dyed under an optical microscope. Group a is the microscope images of S1 cigarette paper with saturation factor 2.0 and brightness gain factor 1.5 after Herzberg staining. Group b is the microscope image of S1 cigarette paper stained with Graff "C", when the saturation factor is set to 2.0 and the brightness gain factor is 1.5.

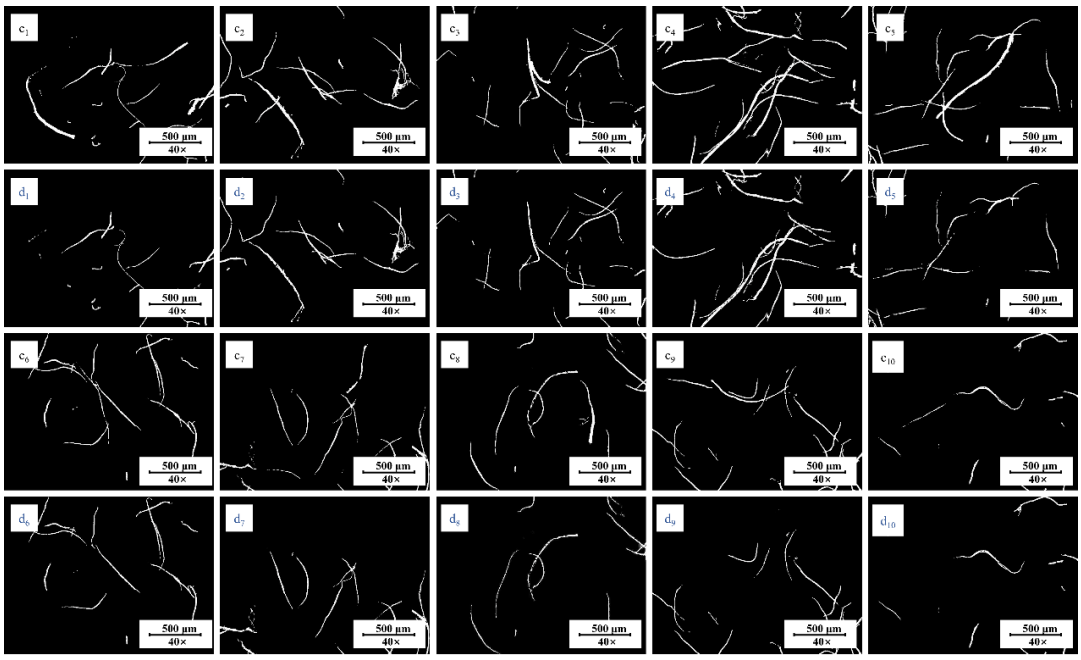

Fig. 17. Images of fibers extracted from sample S1 after Herzberg staining. Here group c is the picture of all fibers extracted, and group d is the picture of hemp pulp fibers separated.

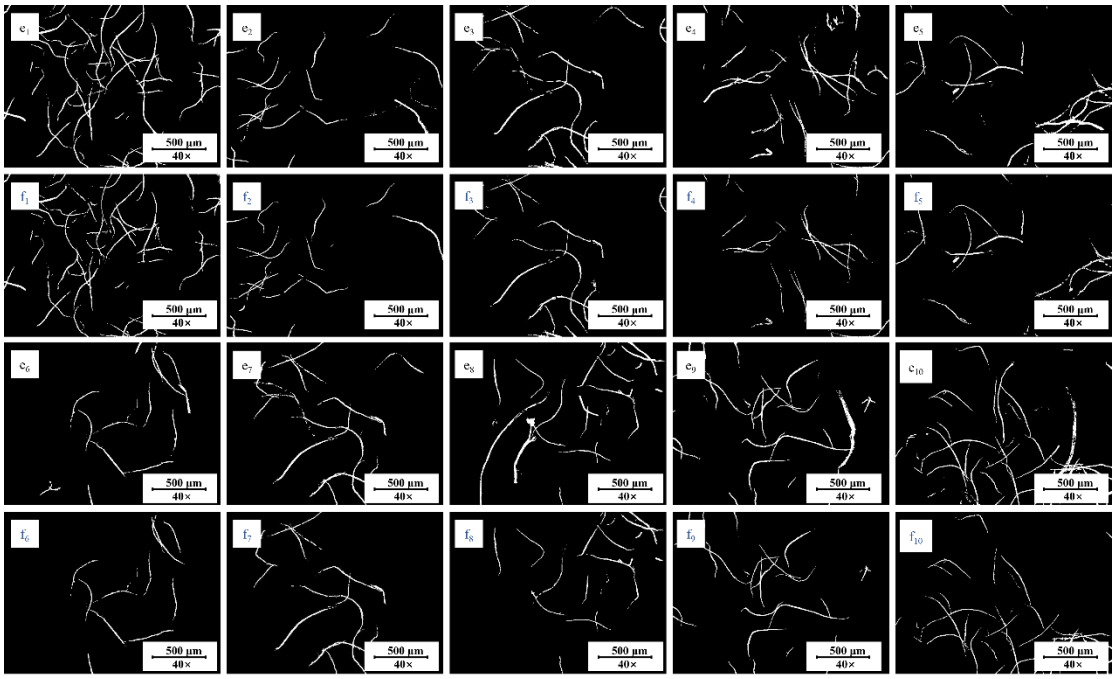

Fig. 18. Images of fibers separated and extracted from S1 sample after Graff"C" staining. Here group e is the picture of all fibers extracted, and group f is the picture of broadleaf fibers extracted.

Herzberg and Graff "C" dyes were diluted to 90% of their standard staining concentrations and stained for 20 s and 30 s, respectively. Images were then captured under an optical microscope (40× and 100×) after staining. Samples of S1 cigarette paper fibers (Figs. 16-18), S2 cigarette paper fibers (Figs. 19, 20), S3 cigarette paper fibers (Figs. 21, 22), S4 cigarette paper fibers (Figs. 23-25), S5 cigarette paper fibers (Figs. 26, 27), S6 cigarette paper fibers (Figs. 28-30), and S7 cigarette paper fibers (Figs. 31 to 33) were analyzed as follows. Ten images stained with Herzberg stain and Graff "C" were selected, respectively, and the obtained fiber images were preprocessed using MATLAB. For Herzberg-stained images, the saturation gain factor was adjusted to 1.5 and the brightness gain factor to 1.1. For Graff "C"-stained images, the saturation gain factor was set to 2.0 and the brightness gain factor to 1.1. The color space was converted into HSV color space, and the color thresholding method was applied to extract all types of fibers and blue fibers after Herzberg-stained (wood pulp fiber), and all types of fibers and blue-gray fibers (hardwood pulp fibers) after Graff "C"-stained. The number of pixels of different types of fibers was counted, and the relevant mass ratios were calculated.

Based on the calculation and analysis, the fiber composition of the dissociated pure fibers in S1 cigarette paper was as follows: Hemp pulp fibers accounted for 23.3%, hardwood fibers for 54.1%, and softwood fibers for 22.5%.

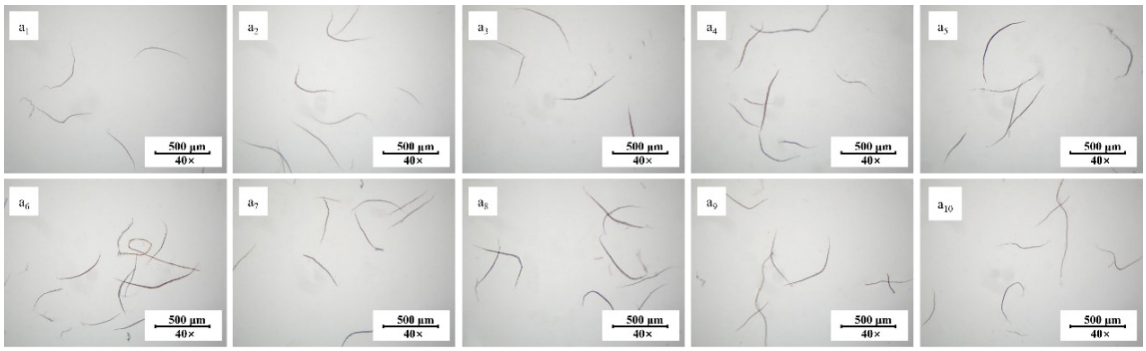

Fig. 19. Image of S2 cigarette paper dyed with Graff“C” was taken under an optical microscope. Group a is the microscope image of S2 cigarette paper stained with Graff "C", when the saturation factor is set to 2.0 and the brightness gain factor is 1.5.

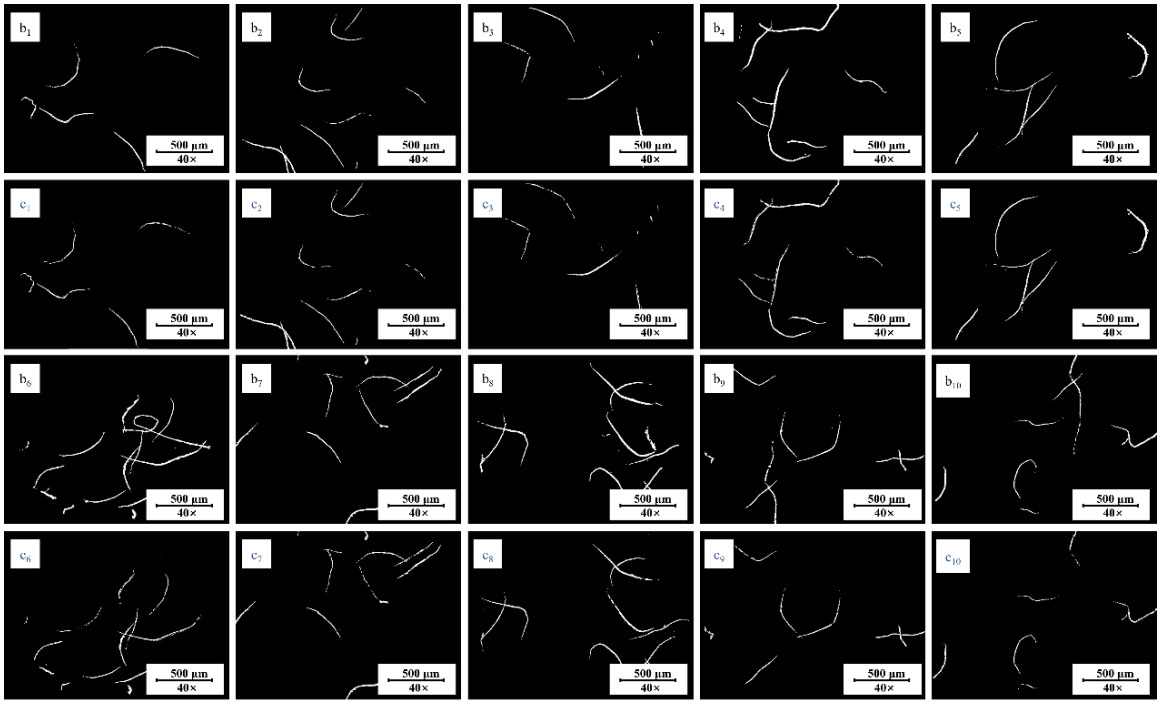

Fig. 20. Images of fibers separated and extracted from S2 sample after Graff“C” staining. Here group b is the picture of all fibers extracted, and group c is the picture of broadleaf fibers extracted.

MATLAB was used to calculate the total pixel count of hardwood fibers and all fibers. Applying Eqs. 2 and 3, the calculated fiber composition of dissociated pure fibers in S2 cigarette paper was 41.7% hardwood fibers and 58.3% softwood fibers.

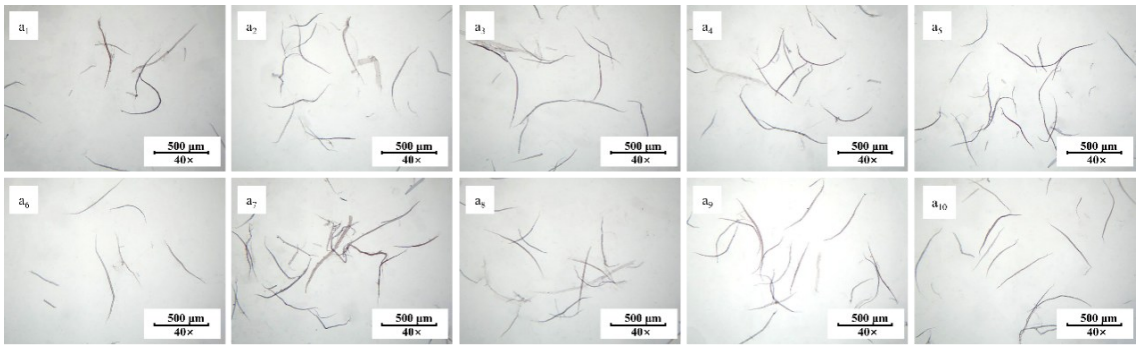

Fig. 21. Image of S3 cigarette paper dyed with Graff“C” was taken under an optical microscope. Group a is the microscope image of S3 cigarette paper stained with Graff "C", when the saturation factor is set to 2.0 and the brightness gain factor is 1.5.

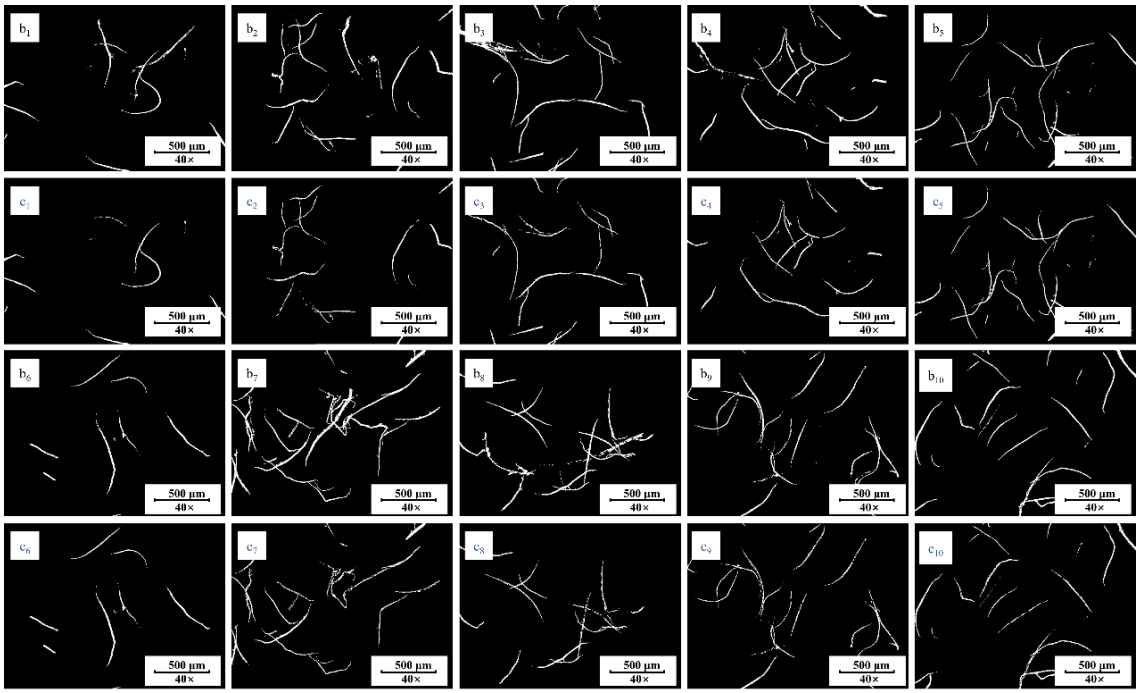

Fig. 22. Images of fibers separated and extracted from S3 sample after Graff“C” staining. Here group b is the picture of all fibers extracted, and group c is the picture of broadleaf fibers extracted.

Since sample S3 is a wood pulp-based paper, no hemp pulp fibers were present. So, MATLAB was used to calculate the pixel count of hardwood fibers and all fibers. Applying Eqs. 2 and 3, the calculated composition of dissociated pure fibers in S3 cigarette paper was 47.89% hardwood fibers and 52.11% softwood fibers.

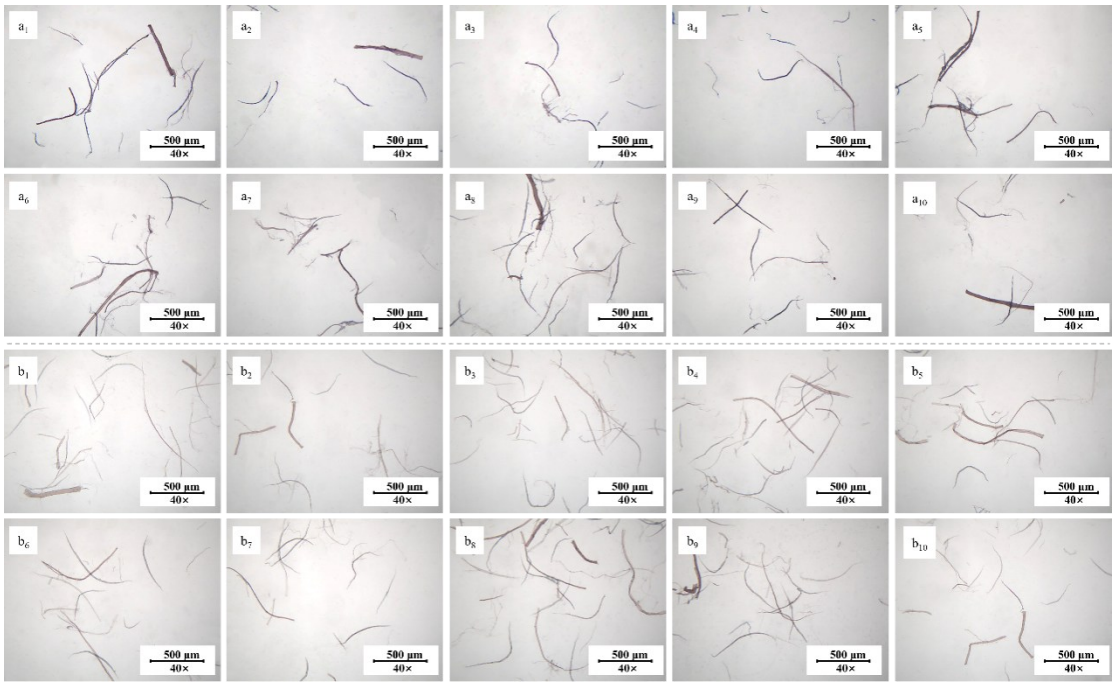

Fig. 23. Image of S4 cigarette paper dyed under an optical microscope. Group a is the microscope images of S4 cigarette paper with saturation factor 2.0 and brightness gain factor 1.5 after Herzberg staining. Group b is the microscope image of S4 cigarette paper stained with Graff "C", when the saturation factor is set to 2.0 and the brightness gain factor is 1.5.

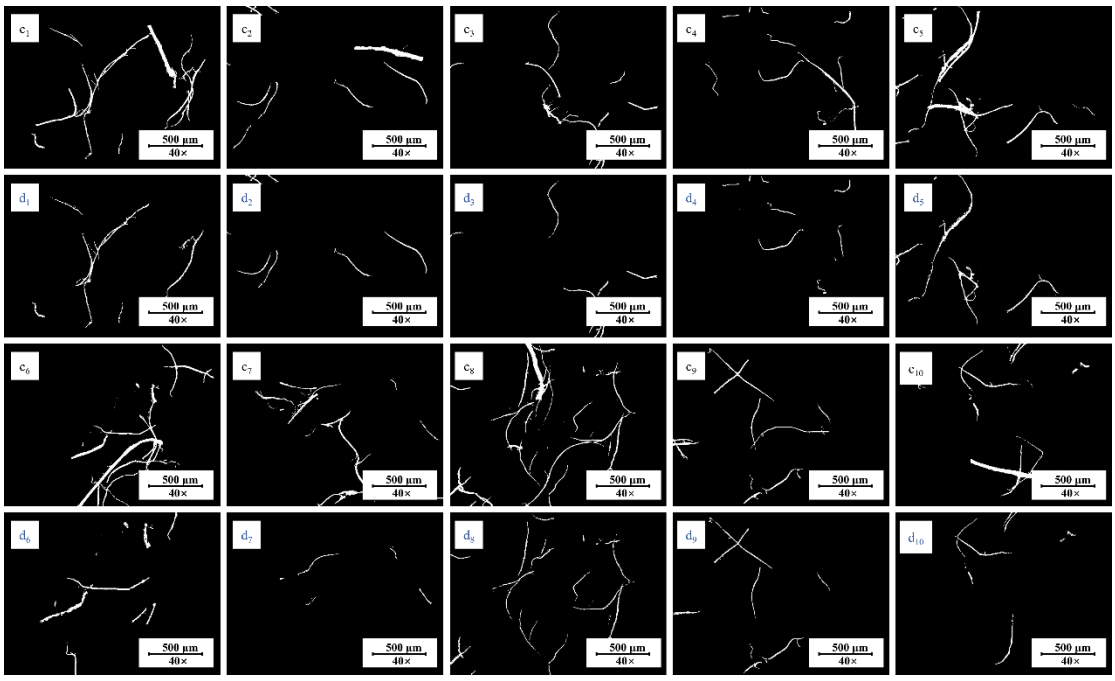

Fig. 24. Images of fibers extracted from sample S4 after Herzberg staining. Here group c is the picture of all fibers extracted, and group d is the picture of hemp pulp fibers separated.

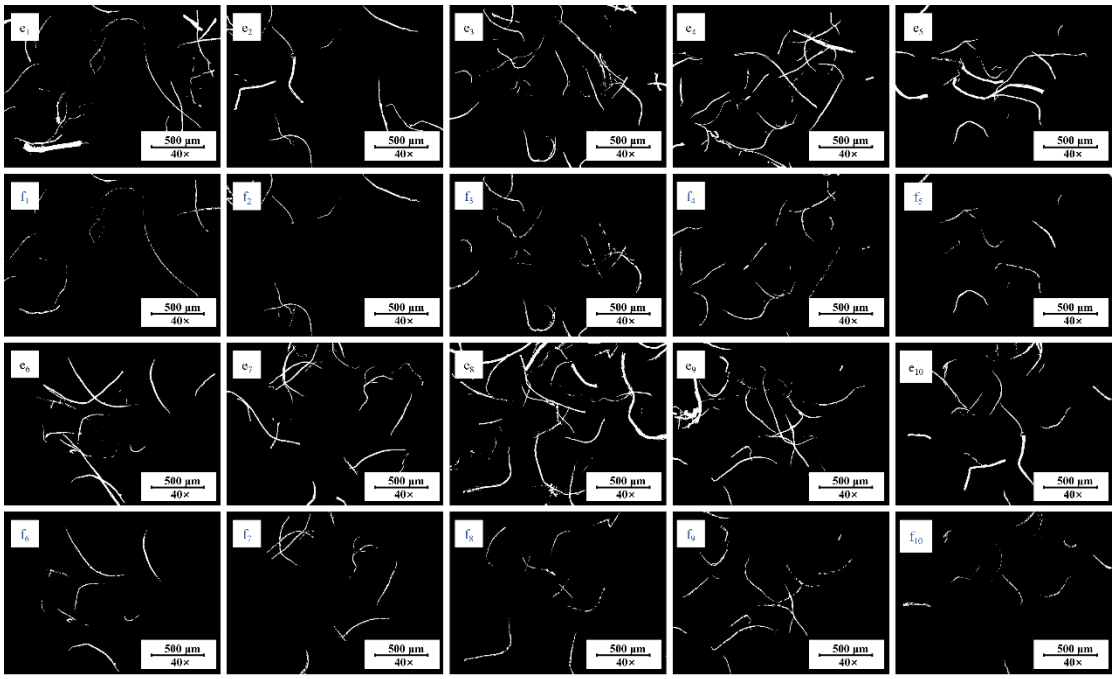

Fig. 25. Images of fibers separated and extracted from S4 sample after Graff"C" staining. Here group e is the picture of all fibers extracted, and group f is the picture of broadleaf fibers extracted.

Sample S4 is a hemp fiber-containing sample. Pixel counts of different fiber types were calculated separately for Herzberg- and Graff "C"-stained images using MATLAB. Based on Eqs. 2 and 3, the calculated fiber composition was 71.9% Hemp pulp fibers, 22.5% hardwood pulp fibers, and 5.6% softwood pulp fibers.

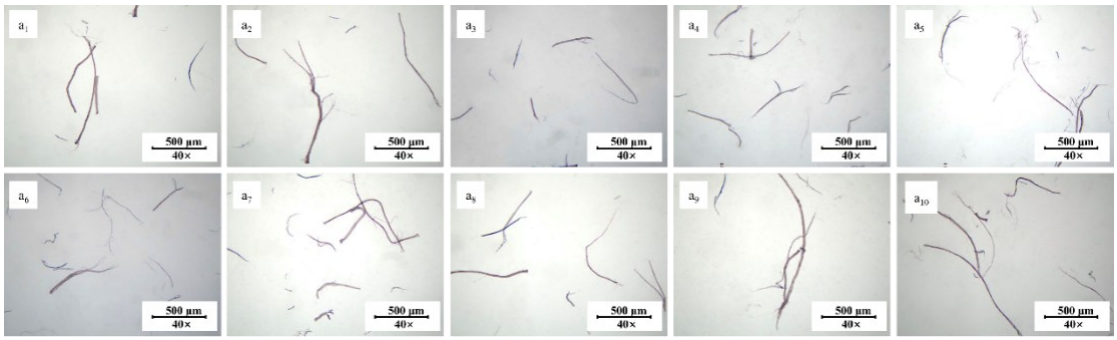

Fig. 26. Image of S5 cigarette paper dyed with Herzberg was taken under an optical microscope. Group a is the microscope images of S5 cigarette paper with saturation factor 2.0 and brightness gain factor 1.5 after Herzberg staining.

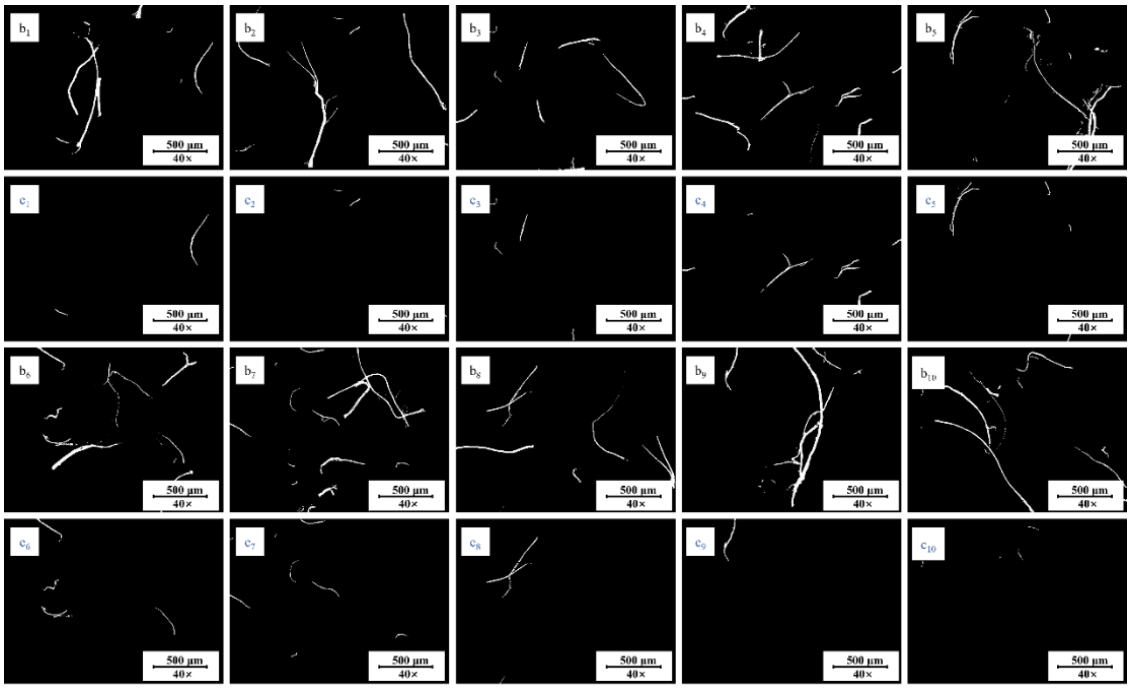

Fig. 27. Images of fibers extracted from sample S5 after Herzberg staining. Here group c is the picture of all fibers extracted, and group d is the picture of hemp pulp fibers separated.

Using MATLAB, the pixel counts of different fiber types were calculated. Applying Eqs. 1 and 2, the calculated Hemp pulp fiber composition in S5 cigarette paper was 96.89%.

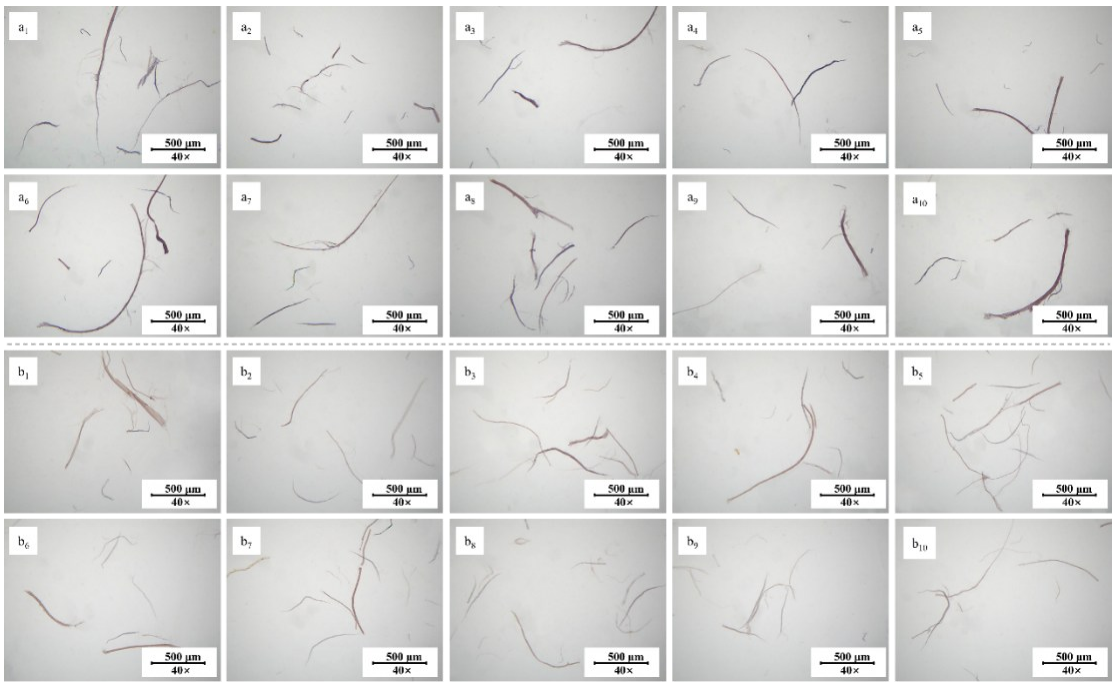

Fig. 28. Image of S6 cigarette paper dyed under an optical microscope. Group a is the microscope images of S6 cigarette paper with saturation factor 2.0 and brightness gain factor 1.5 after Herzberg staining. Group b is the microscope image of S6 cigarette paper stained with Graff "C", when the saturation factor is set to 2.0 and the brightness gain factor is 1.5.

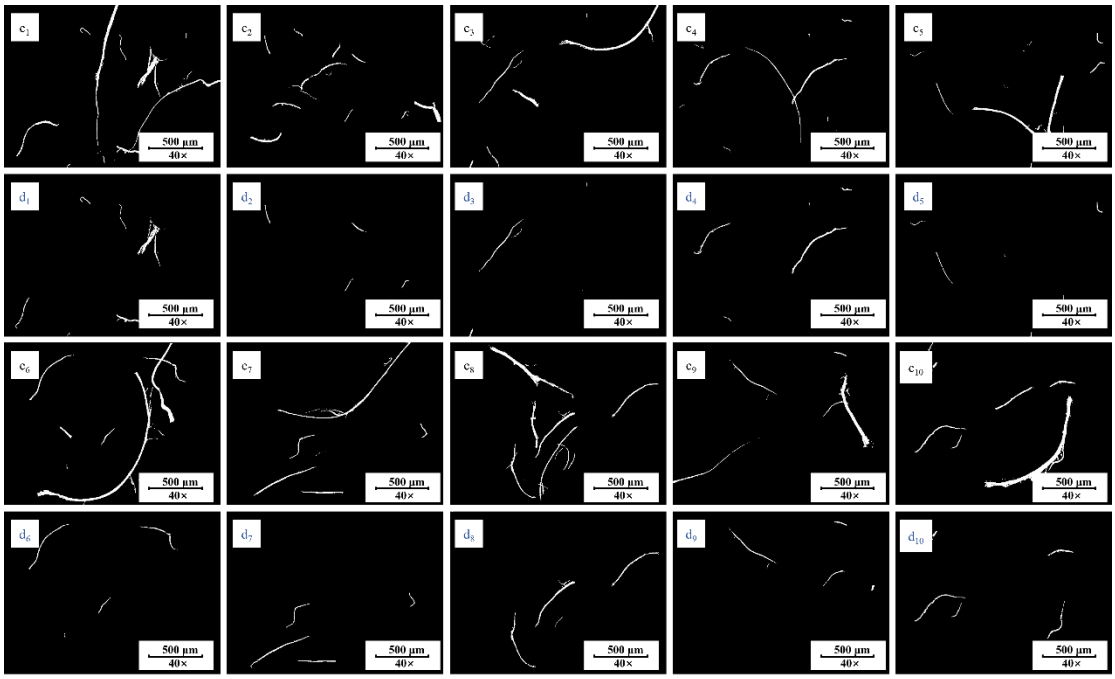

Fig. 29. Images of fibers extracted from sample S6 after Herzberg staining. Here group c is the picture of all fibers extracted, and group d is the picture of hemp pulp fibers separated.

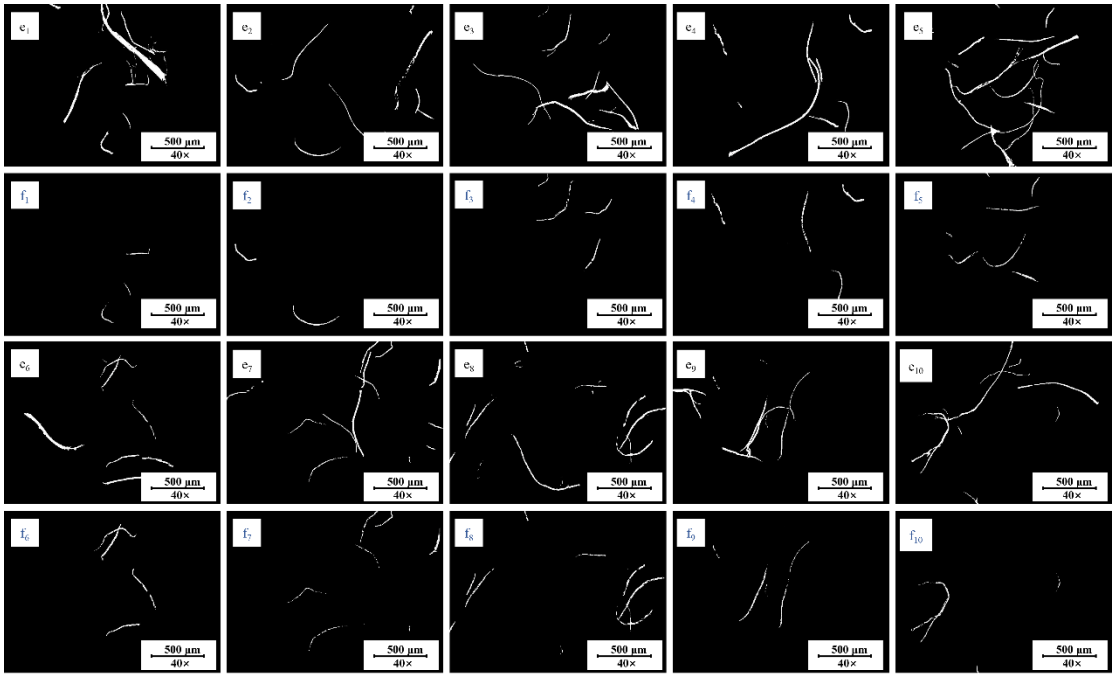

Fig. 30. Images of fibers separated and extracted from S6 sample after Graff"C" staining. Here group e is the picture of all fibers extracted, and group f is the picture of broadleaf fibers extracted).

The pixel counts of different fiber types when calculated after applying Eqs. 1 and 2, the fiber composition in S6 cigarette paper was 81.1% hemp fibers and 18.5% hardwood fibers.

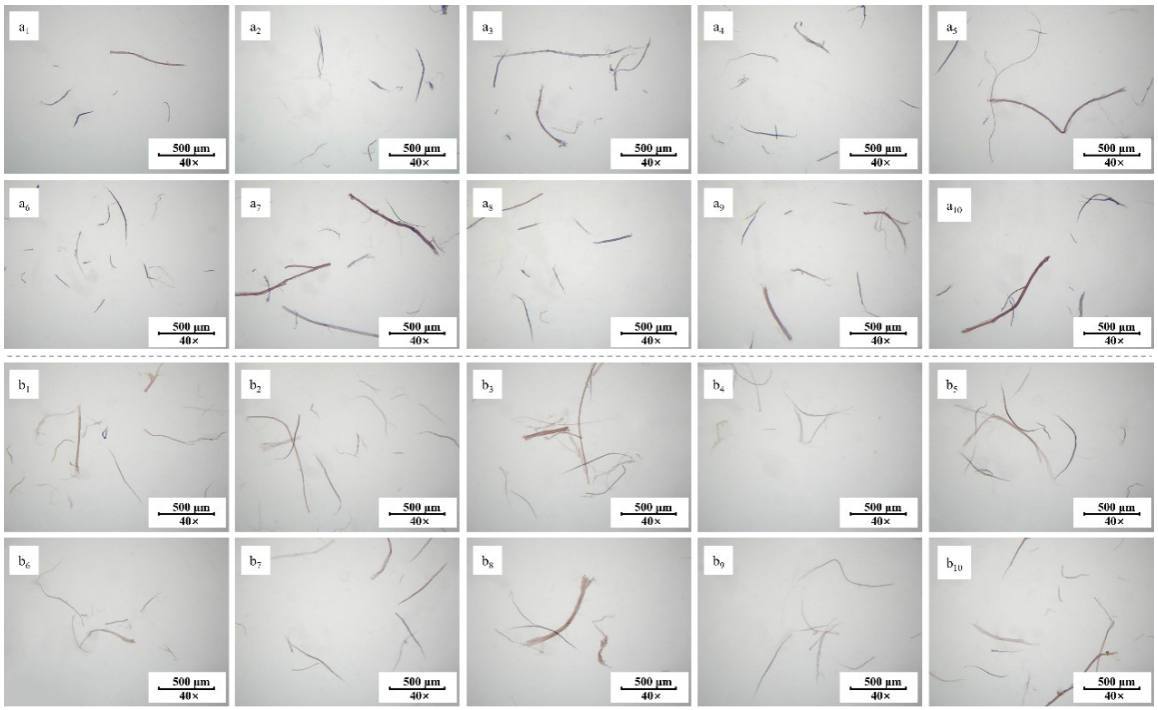

Fig. 31. Image of S7 cigarette paper dyed under an optical microscope. Group a is the microscope images of S7 cigarette paper with saturation factor 2.0 and brightness gain factor 1.5 after Herzberg staining. Group b is the microscope image of S7 cigarette paper stained with Graff "C", when the saturation factor is set to 2.0 and the brightness gain factor is 1.5.

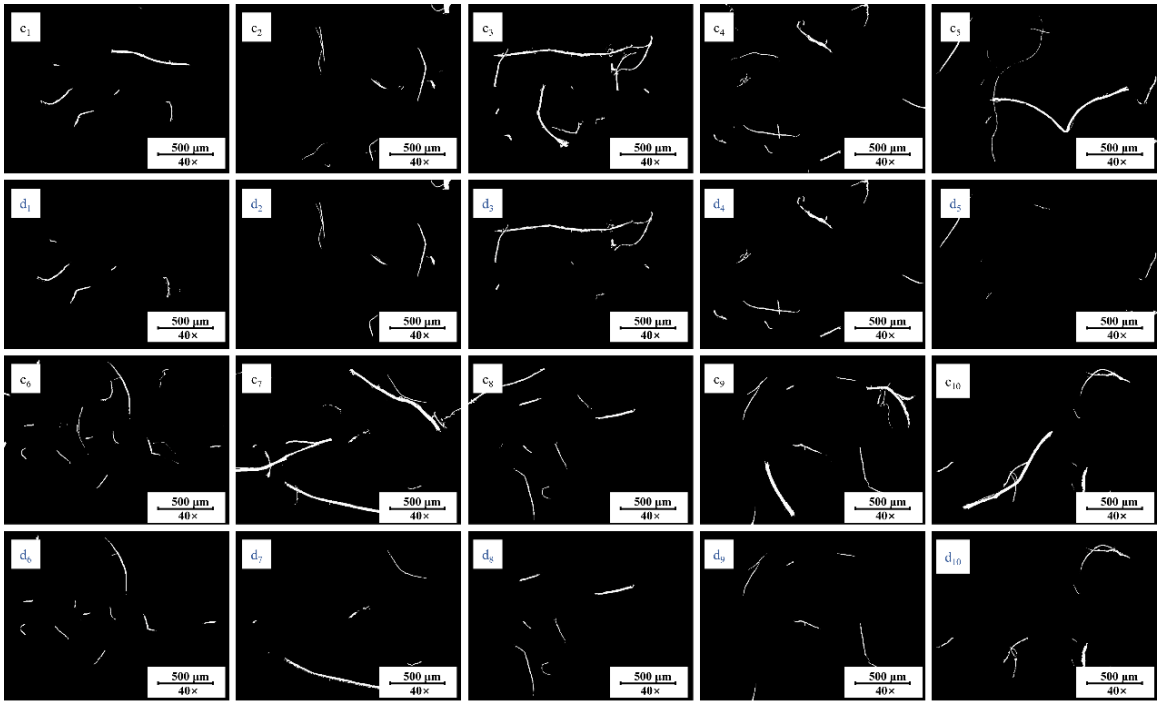

Fig. 32. Images of fibers extracted from sample S7 after Herzberg staining. Here group c is the picture of all fibers extracted, and group d is the picture of hemp pulp fibers separated.

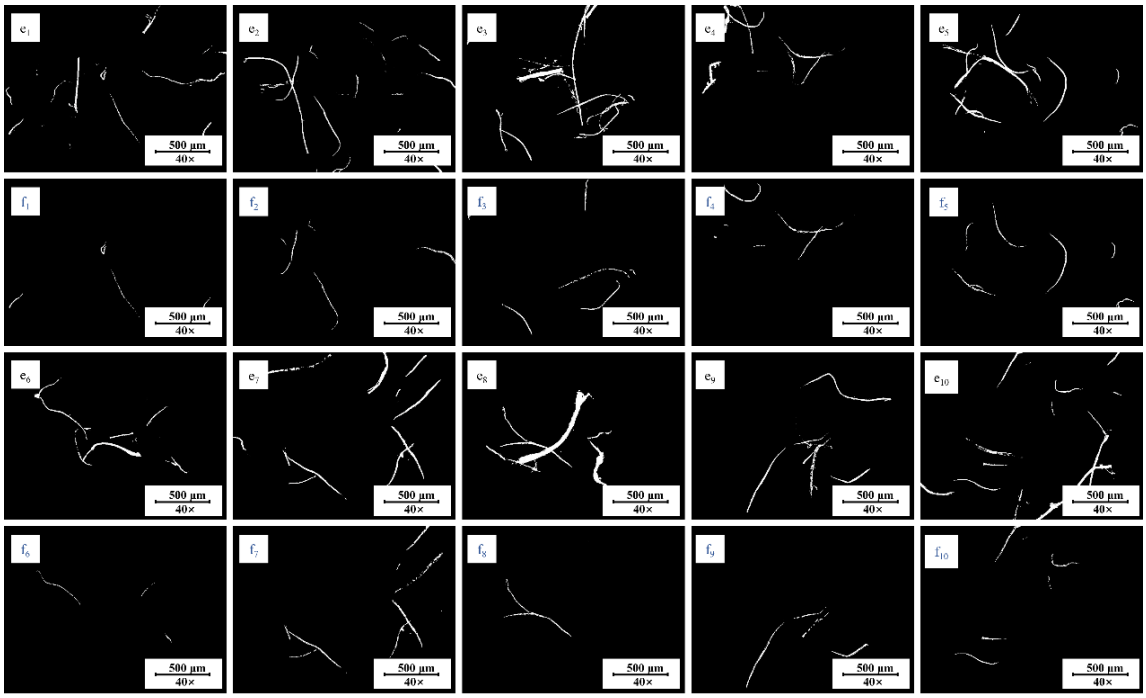

Fig. 33. Images of fibers separated and extracted from S7 sample after Graff"C" staining. Here group e is the picture of all fibers extracted, and group f is the picture of broadleaf fibers extracted).

MATLAB was used to calculate the pixel counts of different fiber types. Applying Eqs. 2 and 3, the calculated fiber composition in S7 cigarette paper was 54.8% hemp pulp fibers, 31.4% hardwood fibers, and 13.9% softwood fibers.

In summary, the results demonstrate the feasibility of this method for practical analysis. Furthermore, this approach significantly improves analytical time efficiency, indicating its high potential for real-world applications.

Accuracy Evaluation of the Staining Method Combined with the Image Recognition Method

In the current field of fiber composition analysis, traditional methods often rely on a single staining reagent combined with optical microscopy or semi-automated measurements, such as ImageJ software (Hubbe *et al.* 2019). These methods generally face multiple limitations, such as reliance on human expertise and low processing efficiency. As shown in Tables 5 and 6, comparing the accuracy of the staining method combined with the image recognition method with traditional methods, it was found that there were no significant differences between the two. However, the former enabled precise separation of hardwood, hemp, and softwood fibers through threshold segmentation, effectively overcoming the subjectivity caused by manual interpretation. In addition, although fiber characteristics and overlapping fibers may affect the segmentation performance, this study maintained a high level of analytical accuracy in mixed pulp systems by preprocessing the images captured by an optical microscope (adjusting the saturation and brightness gain factors).

It is worth noting that, compared to ImageJ software, this method significantly reduces the analysis time. ImageJ requires manual measurement of the length of each fiber (> 200 fibers), often taking several hours per sample, while the threshold segmentation

method only requires threshold segmentation on 10 stained fiber images. The advantage of this method is that it enables high-throughput analysis and enhances the level of data processing.

Table 5. Analysis and Comparison of Accuracy of Two Methods

	Sample ID	Dye-ImageJ Method Accuracy (%)	Dye-Image Recognition Accuracy (%)	Difference (±%)
Softwood and Hardwood Mixture	1	88.1	85.9	2.2
	2	90.9	88.1	2.8
Softwood and Hemp Fiber Mixture	3	93.1	94.9	1.8
	4	99.9	98.1	1.9
Softwood-Hardwood-Hemp Fiber Mixture	5	92.2	93.3	1.0
	6	94.3	93.1	1.2

CONCLUSIONS

1. To overcome the efficiency bottleneck of traditional staining analysis methods that rely on manual counting, this study developed a color threshold segmentation method using MATLAB, extracted color features, and classified fibers from stained microscopic images.
2. Fiber separation and extraction were achieved by transforming the hexagonal cone model, and mass ratios were calculated based on pixel count statistics. The feasibility of this technique in fiber composition analysis was evaluated, showing that the accuracy exceeded 85% in two-component systems and surpassed 90% in three-component systems.
3. Furthermore, the method was applied to the analysis of the fiber composition of seven unknown commercially available cigarette papers, confirming its feasibility in practical applications. This method enables the rapid quantification of fiber components through color feature extraction and pixel counting, providing an efficient technical solution for fiber quality control in industries such as tobacco and papermaking, and has significant prospects for industrial application.

ACKNOWLEDGMENTS

This work was supported by External Cooperation Science and Technology Project of China Tobacco Jiangsu Industrial Co., Ltd. (No. H202229).

REFERENCES CITED

Abd Elaziz, M., Nabil, N., Moghdani, R., Ewees, A. A., Cuevas, E., and Lu, A. (2021). "Multilevel thresholding image segmentation based on improved volleyball premier

league algorithm using whale optimization algorithm," *Multimedia Tools and Applications* 80, 12435-12468. https://doi.org/10.1007/s11042-020-10313-w

Abdelkader, M. (2022). "MATLAB algorithms for diameter measurements of textile yarns and fibers through image processing techniques," *Materials* 15, article 1299. https://doi.org/10.3390/ma15041299

Belyaev, O. F., Zavaruev, V. A., Kudryavin, L. A., and Shablygin, M. V. (2010). "Calculation of the deformation properties of materials made of chemical fibres," *Fibre Chemistry* 41, 276-280. https://doi.org/10.1007/s10692-010-9178-y

Chokshi, S., Parmar, V., Gohil P., and Chaudhary, V. (2020). "Chemical composition and mechanical properties of natural fibers," *Journal of Natural Fibers* 19, 3942-3953. https://doi.org/10.1080/15440478.2020.1848738

Cinko, U. O., and Becerir, B. (2024). "Computing characteristics of color difference formulas for regular coordinate changes in CIELAB color space," *Textile Research Journal* 95(11-12). https://doi.org/10.1177/00405175241278025

Gonzalez, R. C., and Woods, R. E. (2018). *Digital Image Processing*, 4th Ed., Pearson.

He, T., and Li, X. (2019). "Image quality recognition technology based on deep learning," *Journal of Visual Communication and Image Representation* 65, article 102654. https://doi.org/10.1016/j.jvcir.2019.102654

Hubbe, M. A., Chandra, R. P., Dogu, D., and van Velzen, S. T. J. (2019). "Analytical staining of cellulosic materials: A review," *BioResources* 14(3), 7387-7464. https://doi.org/10.15376/biores.14.3.7387-7464

Jraissati, Y., and Douven I. (2018). "Delving deeper into color space," *i-Perception* 9, article 1-27. https://doi.org/10.1177/2041669518792062

Li, Z, H., Dun, X, J., Guang, X, L., Qi, X., Lian, Z., Jin, X. J., and Zou, J. X. (2023). "The types of fibers and pulping methods of modern and contemporary book and periodical paper were examined in two steps based on the dyeing method," *Chinese Journal of Forensic Sciences* 2, article 82-87. https://doi.org/10.3969/j.issn.1671-2072.2023.02.011

Liu, C., Shu X., Pan, L., Shi, J., and Han, B. (2023). "Multiscale underwater image enhancement in RGB and HSV Color Spaces," *IEEE Transactions on Instrumentation and Measurement* 72, article 1-14. DOI: 10.1109/tim.2023.3298395

Liu, X. (2011). "Research progress on the application of plant components in cigarettes," *China Science and Technology Information* 1, article I0064-I0065.

Mo, X., and Chen, T. (2021). "Research on image preprocessing for iris recognition," *Journal of Physics Conference Series* 2031, article 012024. https://doi.org/10.1088/1742-6596/2031/1/012024

Murphy, R., Turcott, A., Banuelos, L., Dowe, E., Goodwin, B., and Cardinal, K. (2020). "SIMPoly: A Matlab-based image analysis tool to measure electrospun polymer scaffold fiber diameter," *Tissue Engineering Part C Methods* 26, article 628-636. https://doi.org/10.1089/ten.tec.2020.0304

National Technical Committee for Standardization of the Paper Industry (SAC/TC 141) (2021). "Determination of mass factor in fiber composition analysis of paper, paperboard and pulp: GB/T 40442-2021," *China Standards Press*.

Newell, B. D. (2020). "Understanding digital color imaging and processing," *Microscopy and Microanalysis* 4, article 56-57. https://doi.org/10.1017/s1431927600020407

Robertson, S., Azizpour, H., Smith, K., and Hartman, J. (2017). "Digital image analysis in breast pathology-from image processing techniques to artificial intelligence," *Translational research* 194, article 19-35. https://doi.org/10.1016/j.trsl.2017.10.010

Ruan, R., Cao, W., and Xu, L. (2020). "Quantitative characterization of physical structure on carbon fiber surface based on image technique," *Materials & Design* 185, article 108225. https://doi.org/10.1016/j.matdes.2019.108225

Sun, Y., and Zhang, C, X. (2021). "Qualitative analysis methods for Herzberg dyeing of different papermaking fiber raw materials," *Paper Chemicals* 1, article 19-22.

Tadahiro, A., Ayaka, F., and Noriaki, S. (2024). "Image enhancement for dichromatic vision by geometric approach in RGB color space," *Color Research and Application* 50, article 125-131. https://doi.org/10.1002/col.22956

Vohra, S. K., and Prodanov, D. (2021). "The active segmentation platform for microscopic image classification and segmentation," *Brain Sciences* 11, article 1645. https://doi.org/10.3390/brainsci11121645

Vyas, A., Yu, S., and Paik, J. (2018). "Multiscale transforms with application to image processing," *Signals and Communication Technology*. https://doi.org/10.1007/978-981-10-7272-7

Xing, W., Deng, N., Xin, B., Wang, Y., Chen, Y., and Zhang, Z. (2019). "An image-based method for the automatic recognition of cashmere and wool fibers," *Measurement* 141, article 102-112. https://doi.org/10.1016/j.measurement.2019.04.015

Zhang, Y., and Dong, Z. (2016). "Simulation of digital image processing in medical applications," *Simulation* 92, article 825-826. https://doi.org/10.1177/0037549716670053

Zortea, M., Flores, E., Scharcanski, J. (2017). "A simple weighted thresholding method for the segmentation of pigmented skin lesions in macroscopic images," *Pattern Recognition* 64, article 92-104. https://doi.org/10.1016/j.patcog.2016.10.031

Article submitted: July 25, 2025; Peer review completed: October 25, 2025; Revised version received and accepted: February 28, 2026; Published: April 1, 2026.
DOI: 10.15376/biores.21.2.4408-4435